



日本原子力研究開発機構機関リポジトリ  
Japan Atomic Energy Agency Institutional Repository

Title	Electromagnetic transitions of the singly charmed baryons with spin 3/2
Author(s)	Kim J.-Y., Kim H.-C., Yang G.-S., Oka Makoto
Citation	Physical Review D,103(7),p.074025_1-074025_21
Text Version	Published Journal Article
URL	<a href="https://jopss.jaea.go.jp/search/servlet/search?5070842">https://jopss.jaea.go.jp/search/servlet/search?5070842</a>
DOI	<a href="https://doi.org/10.1103/PhysRevD.103.074025">https://doi.org/10.1103/PhysRevD.103.074025</a>
Right	Published by the American Physical Society under the terms of the Creative Commons Attribution 4.0 International license. Further distribution of this work must maintain attribution to the author(s) and the published article's title, journal citation, and DOI. Funded by SCOAP <sup>3</sup> .

**Electromagnetic transitions of the singly charmed baryons with spin 3/2**June-Young Kim,<sup>1,2,\*</sup> Hyun-Chul Kim<sup>2,3,†</sup> Ghil-Seok Yang,<sup>4,‡</sup> and Makoto Oka<sup>5,§</sup><sup>1</sup>*Institut für Theoretische Physik II, Ruhr-Universität Bochum, D-44780 Bochum, Germany*<sup>2</sup>*Department of Physics, Inha University, Incheon 22212, Republic of Korea*<sup>3</sup>*School of Physics, Korea Institute for Advanced Study (KIAS), Seoul 02455, Republic of Korea*<sup>4</sup>*Department of General Education for Human Creativity, Hoseo University, Asan 31499, Republic of Korea*<sup>5</sup>*Advanced Science Research Center, Japan Atomic Energy Agency, Shirakata, Tokai, Ibaraki 319-1195, Japan*

(Received 26 January 2021; accepted 30 March 2021; published 28 April 2021)

We investigate the electromagnetic transitions of the singly charmed baryons with spin 3/2, based on a pion mean-field approach, also known as the chiral quark-soliton model, taking into account the rotational  $1/N_c$  corrections and the effects of flavor SU(3) symmetry breaking. We examine the valence- and sea-quark contributions to the electromagnetic transition form factors and find that the quadrupole form factors of the sea-quark contributions dominate over those of the valence-quark ones in the smaller  $Q^2$  region, whereas the sea quarks only provide marginal contributions to the magnetic dipole transition form factors of the baryon sextet with spin 3/2. The effects of the flavor SU(3) symmetry breaking are in general very small except for the forbidden transition  $\Xi_c^0 \gamma \rightarrow \Xi_c^{*0}$  by  $U$ -spin symmetry. We also discuss the widths of the radiative decays for the baryon sextet with spin 3/2, comparing the present results with those from other works.

DOI: 10.1103/PhysRevD.103.074025

**I. INTRODUCTION**

It is of great importance to understand the electromagnetic (EM) structure of a baryon, since it reveals how the baryon is shaped by its constituents. A baryon with spin 3/2 has a finite value of the electric quadrupole (E2) moment, which indicates that its charge distribution is shown to be deformed to be either a cushionlike form (oblate spheroid) or a rugby-ball-like one (prolate spheroid), depending on the signature of its charge in the body-fixed frame [1]. This implies that a singly heavy baryon with spin 3/2 may reveal a similar structure. It is also known that the effects of the vacuum polarization or those of the pion clouds are known to contribute significantly to the E2 moment of the baryon decuplet [2]. This leads to an interpretation that the E2 moment of a low-lying baryon with spin 3/2 is governed by long-distance pion clouds [3]. While experimental information on the EM transitions of

the singly heavy baryons is still inconclusive [4–7], there has been a great deal of theoretical work within many different approaches such as chiral perturbation theory [8–12], the quark models [13–15], QCD sum rules [16–18], and so on (see also a recent review [19]). In lattice QCD, the EM transition form factors for  $\Omega_c^0 \gamma \rightarrow \Omega_c^{*0}$  were calculated [20,21]. Thus, anticipating that the experimental data on the EM transitions of the singly heavy baryons will be available in the near future, it is of great interest to investigate the structure of the EM transition form factors in a different theoretical framework.

In the present work, we investigate the EM transition form factors of the low-lying singly heavy baryons with spin 3/2 within the framework of the chiral quark-soliton model ( $\chi$ QSM). The model is based on a pion mean-field approach. As was proposed first by Witten [22], in the large  $N_c$  limit, the light baryon can be viewed as a state of  $N_c$  (the number of colors) valence quarks bound by the pion mean fields that have been produced self-consistently by the  $N_c$  valence quarks [23,24]. The model was extended to the description of the singly heavy baryons [25–27], being motivated by Ref. [28]. In the limit of the infinitely heavy quark mass ( $m_Q \rightarrow \infty$ ), the spin of the heavy quark cannot be flipped, which makes the heavy-quark spin conserved. This causes also the total spin of the light quarks inside a singly heavy baryon conserved. In this limit of  $m_Q \rightarrow \infty$ , the flavor of the heavy quark does not come into play. This

\*Jun-Young.Kim@ruhr-uni-bochum.de

†hchkim@inha.ac.kr

‡ghsyang@ssu.ac.kr

§oka@post.j-parc.jp

Published by the American Physical Society under the terms of the [Creative Commons Attribution 4.0 International license](https://creativecommons.org/licenses/by/4.0/). Further distribution of this work must maintain attribution to the author(s) and the published article's title, journal citation, and DOI. Funded by SCOAP<sup>3</sup>.

is known as the heavy-quark spin-flavor symmetry [29–31]. Thus, the singly heavy baryons can be expressed within the SU(3) representations. That is, two light valence quarks ( $\mathbf{3} \otimes \mathbf{3}$ ) will allow one to have the baryon antitriplet ( $\bar{\mathbf{3}}$ ) and sextet ( $\mathbf{6}$ ). The spins of the two light valence quarks can be aligned either in the spin-singlet state ( $\mathbf{0}$ ) or in the spin-triplet one ( $\mathbf{1}$ ). Hence, by combining them with the spin of the heavy quark, one can have two degenerate baryon sextets. This degeneracy can be removed by the color hyperfine interaction in order  $1/m_Q$  [25]. Note that the infinitely heavy quark can be regarded as the mere static color source. This indicates that the light quarks govern the dynamics inside a singly heavy baryon. Based on this heavy-quark spin-flavor symmetry, the pion mean-field approach was developed also for the singly heavy baryons that can be regarded as the bound state of  $N_c - 1$  valence quarks. The heavy quark inside a singly heavy baryon is required only for the construction of a color-singlet state of the singly heavy baryon.

This pion mean-field approach or the  $\chi$ QSM described various properties of the singly heavy baryons quantitatively well, compared with the experimental data, without any free parameters [25–27,32–35] (see also a recent review [36]). The EM form factors of the low-lying singly heavy baryons have been studied in the  $\chi$ QSM [37,38]. Since the heavy-quark mass is taken to be infinitely heavy, the heavy quark gives a constant contribution to the electric monopole form factor constrained by the gauge invariance, whereas contributions to the magnetic dipole form factor from the heavy quark is negligible. The numerical results were in good agreement with the lattice data [39]. In the present work, we want to investigate the EM transition form factors of the baryon sextet with spin 3/2. While the  $\Omega_c^0 \gamma \rightarrow \Omega_c^{*0}$  radiative decay was computed in lattice QCD, there is no work on the EM transition form factors for all possible radiative decays for the baryon sextet with spin 3/2. Thus, we will consider for the first time the magnetic dipole (M1) and electric quadrupole and Coulomb quadrupole (C2) transition form factors for the baryon sextet ( $\mathbf{6}$ ) with spin 3/2. We will compare the results for the  $\Omega_c^0 \gamma \rightarrow \Omega_c^{*0}$  radiative decay with those from the lattice calculation. We will compare the present numerical results for the decay rates of the radiative decays for the singly heavy baryons with those from other theoretical works.

The present work is organized as follows. In Sec. II, we define the M1, E2, and C2 transition form factors of the singly heavy baryons. In Sec. III, we explain explicitly how the singly heavy baryon state can be consistently constructed based on the heavy-quark spin-flavor symmetry in the limit of the infinitely heavy-quark mass. We show that the heavy-quark field can be decoupled from the singly heavy baryon and its mass contributes to the classical mass of the singly heavy baryon in a simple manner. In Sec. IV, we show briefly how to compute them within the framework of the  $\chi$ QSM. In Sec. V, we first compare the numerical results

for  $\Omega_c + \gamma \rightarrow \Omega_c^*$  with those of the corresponding lattice data. We also examine the dependence of the EM transition form factors of  $\Omega_c + \gamma \rightarrow \Omega_c^*$  on the pion mass. We then scrutinize the valence- and sea-quark contributions separately and show that the sea quarks or the Dirac continuum play a crucial role in describing the E2 and C2 transition form factors of the baryon sextet with spin 3/2, which can be interpreted as the pion clouds. We also study the effects of the explicit breaking of flavor SU(3) symmetry breaking on the EM transition form factors of the baryon sextet with spin 3/2. We compare the present results for the decay rates of the radiative decays for the singly heavy baryons with spin 3/2 with those from other works. Finally, we summarize the results from the present work and draw conclusions.

## II. EM TRANSITION FORM FACTORS OF THE BARYON SEXTET WITH SPIN 3/2

To describe the EM transition from a singly heavy baryon with spin 1/2 to that with spin 3/2,  $B\gamma^* \rightarrow B^*$ , we assume that the baryon with spin 3/2 is at rest. In this rest frame, we define the 4-momenta for the baryon with spin 3/2, the baryon with spin 1/2, and the photon, respectively, as  $p_{B^*}$ ,  $p_B$ , and  $q$ , which are explicitly written as

$$p_{B^*} = (M_{B^*}, \mathbf{0}), \quad p = (E_B, -\mathbf{q}), \quad q = (\omega_q, \mathbf{q}), \quad (1)$$

where  $\mathbf{q}$  and  $\omega_q$  denote the 3-momentum and energy of the virtual photon. The energy-momentum relation is given by  $E_B^2 = M_B^2 + |\mathbf{q}|^2$  and  $E_{B^*}^2 = M_{B^*}^2$ . Using this relation, we can express the momentum and the energy of the virtual photon as

$$|\mathbf{q}|^2 = \left( \frac{M_{B^*}^2 + M_B^2 + Q^2}{2M_{B^*}} \right)^2 - M_B^2, \quad (2)$$

$$\omega_q = \left( \frac{M_{B^*}^2 - M_B^2 - Q^2}{2M_{B^*}} \right),$$

where  $Q^2 = -q^2 > 0$ .

We start with the EM current defined by

$$V^\mu(x) = \bar{\psi}(x)\gamma^\mu \hat{Q}\psi(x) + \bar{\Psi}_h(x)\gamma^\mu Q_h \Psi_h(x), \quad (3)$$

where  $\psi(x)$  and  $\Psi_h(x)$  denote, respectively, the light and heavy quarks. The first term in Eq. (3) is the EM current for the light quarks with the charge operator defined by the charges of the light quarks  $\hat{Q} = \text{diag}(2/3, -1/3, -1/3)$ . The second term represents the EM current for the heavy quark with a heavy-quark charge  $Q_h$ . If one considers the charm quark, then  $Q_h = 2/3$ . In the case of the bottom baryon, we have  $Q_h = -1/3$ . In the present work, we will consider only the charmed baryons. The transition EM matrix element between  $B^*$  and  $B$  is then parametrized in terms of the three real EM transition form factors

$$\langle B^*(p', \lambda') | V^\mu(0) | B(p, \lambda) \rangle = i \sqrt{\frac{2}{3}} \bar{u}_\beta(p', \lambda') \Gamma^{\beta\mu} u(p, \lambda). \quad (4)$$

$\lambda$  and  $\lambda'$  denote the helicities of the baryons with spins 1/2 and 3/2, respectively.  $u_\beta(p, \lambda')$  and  $u(p, \lambda)$  stand for the Rarita-Schwinger and Dirac spinors, respectively.  $\Gamma^{\beta\mu}$  in Eq. (4) denote the three real EM transition form factors,

$$\Gamma^{\beta\mu} = G_{M1}^*(Q^2) \mathcal{K}_{M1}^{\beta\mu} + G_{E2}^*(Q^2) \mathcal{K}_{E2}^{\beta\mu} + G_{C2}^*(Q^2) \mathcal{K}_{C2}^{\beta\mu}, \quad (5)$$

where  $G_{M1}^*$ ,  $G_{E2}^*$ , and  $G_{C2}^*$  are known, respectively, as the magnetic dipole transition form factor, the electric quadrupole one, and the Coulomb quadrupole one. The corresponding Lorentz tensors  $\mathcal{K}_{M1}^{\beta\mu}$  are written as

$$\begin{aligned} \mathcal{K}_{M1}^{\beta\mu} &= \frac{-3(M_{B^*} + M_B)}{2M_B[(M_{B^*} + M_B)^2 + Q^2]} \varepsilon^{\beta\mu\sigma\tau} P_\sigma q_\tau, \\ \mathcal{K}_{E2}^{\beta\mu} &= -\mathcal{K}_M^{\beta\mu} - \frac{6}{4M_{B^*}^2 |q|^2} \frac{M_{B^*} + M_B}{M_B} \varepsilon^{\beta\sigma\nu\gamma} P_\nu q_\gamma \varepsilon^{\mu\alpha\delta} p_{B^* \alpha} q_\delta i\gamma^5, \\ \mathcal{K}_{C2}^{\beta\mu} &= -\frac{3}{4M_{B^*}^2 |q|^2} \frac{M_{B^*} + M_B}{M_B} q^\beta [q^2 P^\mu - q \cdot P q^\mu] i\gamma^5. \end{aligned} \quad (6)$$

The Lorentz tensors are required to satisfy the gauge-invariant identities  $q_\mu \mathcal{K}_{M1, E2, C2}^{\beta\mu} = 0$ , which arises from the conservation of the EM current.

The EM transition form factors can be extracted experimentally by using the helicity amplitudes. The transverse and Coulomb helicity amplitudes are defined, respectively, in terms of the spatial and temporal components of the EM current,

$$\begin{aligned} A_\lambda &= -\frac{e}{\sqrt{2\omega_q}} \int d^3 r e^{iq \cdot r} \epsilon_{+1} \\ &\quad \cdot \langle B^*(3/2, \lambda) | \bar{\psi}(\mathbf{r}) \hat{Q} \gamma \psi(\mathbf{r}) | B(1/2, \lambda - 1) \rangle, \\ S_{1/2} &= -\frac{e}{\sqrt{2\omega_q}} \frac{1}{\sqrt{2}} \int d^3 r e^{iq \cdot r} \\ &\quad \times \langle B^*(3/2, 1/2) | \bar{\psi}(\mathbf{r}) \hat{Q} \gamma^0 \psi(\mathbf{r}) | B(1/2, 1/2) \rangle, \end{aligned} \quad (7)$$

where  $\lambda$  is the corresponding value of the helicity of the baryon  $B^*$  with spin 3/2, i.e.,  $\lambda = 3/2$  or  $1/2$ . Note that the transverse photon polarization vector is defined as  $\hat{\epsilon} = -1/\sqrt{2}(1, i, 0)$ . The helicity amplitudes are expressed in terms of the EM transition form factors

$$\begin{aligned} A_{1/2} &= -\frac{e}{\sqrt{2\omega_q}} \frac{1}{4c_\Delta} (G_{M1}^* - 3G_{E2}^*), \\ A_{3/2} &= -\frac{e}{\sqrt{2\omega_q}} \frac{\sqrt{3}}{4c_\Delta} (G_{M1}^* + G_{E2}^*), \\ S_{1/2} &= \frac{e}{\sqrt{2\omega_q}} \frac{|q|}{4c_\Delta M_{B^*}} G_{C2}^*, \end{aligned} \quad (8)$$

where  $c_\Delta = \sqrt{\frac{M_B^3}{2M_{B^*} |q|^2} \sqrt{1 + \frac{Q^2}{(M_{B^*} + M_B)^2}}$ . Then, we are able to express the EM transition form factors inversely by the transition amplitudes

$$\begin{aligned} G_{M1}^*(Q^2) &= -2c_\Delta \int d^3 r 3j_1(|\mathbf{q}||\mathbf{r}|) \\ &\quad \times \langle B^*(3/2, 1/2) | [\hat{\mathbf{r}} \times \mathbf{V}]_{11} | B(1/2, -1/2) \rangle, \\ G_{E2}^*(Q^2) &\simeq -2c_\Delta \int d^3 r \sqrt{\frac{20\pi \omega_q}{27}} \frac{1}{|q|} \left( \frac{\partial}{\partial r} r j_2(|\mathbf{q}||\mathbf{r}|) \right) \\ &\quad \times \langle B^*(3/2, 1/2) | Y_{21}(\hat{\mathbf{r}}) V_0 | B(1/2, -1/2) \rangle, \\ G_{C2}^*(Q^2) &= 4c_\Delta \frac{M_{B^*}}{|q|} \int d^3 r \sqrt{10\pi} j_2(|\mathbf{q}||\mathbf{r}|) \\ &\quad \times \langle B^*(3/2, 1/2) | Y_{20}(\hat{\mathbf{r}}) V_0 | B(1/2, 1/2) \rangle. \end{aligned} \quad (9)$$

Note that we neglect a term that provides a tiny correction to the E2 transition form factor at low-energy regions, which implements the current conservation.

From the form factors, the well-known quantities  $R_{EM}$  and  $R_{SM}$ , which are defined, respectively, as

$$R_{EM}(Q^2) = -\frac{G_{E2}^*(Q^2)}{G_{M1}^*(Q^2)}, \quad R_{SM}(Q^2) = -\frac{|q|}{2M_{B^*}} \frac{G_{C2}^*(Q^2)}{G_{M1}^*(Q^2)}, \quad (10)$$

can be obtained. The decay width is expressed in terms of the helicity amplitudes [40]

$$\begin{aligned} \Gamma(B^* \rightarrow B\gamma) &= \frac{\omega_q^2}{\pi} \frac{M_B}{2M_{B^*}} (|A_{1/2}|^2 + |A_{3/2}|^2) \\ &= \frac{\alpha_{EM}}{16} \frac{(M_{B^*}^2 - M_B^2)^3}{M_{B^*}^3 M_B^2} (|G_{M1}^*(0)|^2 + 3|G_{E2}^*(0)|^2) \end{aligned} \quad (11)$$

with the EM fine structure constant  $\alpha_{EM}$ .

### III. SINGLY HEAVY BARYON IN THE CHIRAL QUARK-SOLITON MODEL

The pion mean-field approach or the  $\chi$ QSM has one great virtue. The model allows one to describe both light baryons and singly heavy baryons on an equal footing. While various properties of singly heavy baryons were investigated in the previous works based on the  $\chi$ QSM, it was not discussed formally how a singly heavy baryon can be explicitly constructed in the  $\chi$ QSM. Thus, before we compute the EM transition form factors of singly heavy baryons, we first want to show how a singly heavy baryon can be formulated in the present approach. Let us first define the normalization of the baryon state  $\langle B(p', J'_3) | B(p, J_3) \rangle = 2p_0 \delta_{J'_3, J_3} (2\pi)^3 \delta^{(3)}(\mathbf{p}' - \mathbf{p})$ . In the large  $N_c$  limit, this normalization can be expressed as

$\langle B(p', J'_3) | B(p, J_3) \rangle = 2M_B \delta_{J'_3 J_3} (2\pi)^3 \delta^{(3)}(\mathbf{p}' - \mathbf{p})$ , where  $M_B$  is a baryon mass. Since a singly heavy baryon consists of the  $N_c - 1$  valence quarks and a heavy quark, it can be

expressed in terms of the Ioffe-type current of the  $N_c - 1$  valence quarks and a heavy-quark field in Euclidean space as

$$\begin{aligned} |B, p\rangle &= \lim_{x_4 \rightarrow -\infty} \exp(ip_4 x_4) \mathcal{N}(\mathbf{p}) \int d^3x \exp(i\mathbf{p} \cdot \mathbf{x}) (-i\Psi_h^\dagger(\mathbf{x}, x_4) \gamma_4) J_B^\dagger(\mathbf{x}, x_4) |0\rangle, \\ \langle B, p| &= \lim_{y_4 \rightarrow \infty} \exp(-ip'_4 y_4) \mathcal{N}^*(\mathbf{p}') \int d^3y \exp(-i\mathbf{p}' \cdot \mathbf{y}) \langle 0 | J_B(\mathbf{y}, y_4) \Psi_h(\mathbf{y}, y_4), \end{aligned} \quad (12)$$

where  $\mathcal{N}(\mathbf{p})$  ( $\mathcal{N}^*(\mathbf{p}')$ ) stands for the normalization factor depending on the initial (final) momentum.  $J_B(x)$  and  $J_B^\dagger(y)$  denote the Ioffe-type current of the  $N_c - 1$  valence quarks [23] defined by

$$\begin{aligned} J_B(x) &= \frac{1}{(N_c - 1)!} \epsilon_{\alpha_1 \dots \alpha_{N_c-1}} \Gamma_{(TT_3 Y)(JJ_3 Y_R)}^{f_1 \dots f_{N_c-1}} \psi_{f_1 \alpha_1}(x) \dots \psi_{f_{N_c-1} \alpha_{N_c-1}}(x), \\ J_B^\dagger(y) &= \frac{1}{(N_c - 1)!} \epsilon_{\alpha_1 \dots \alpha_{N_c-1}} \Gamma_{(TT_3 Y)(JJ_3 Y_R)}^{f_1 \dots f_{N_c-1}} (-i\psi^\dagger(y) \gamma_4)_{f_1 \alpha_1} \dots (-i\psi^\dagger(y) \gamma_4)_{f_{N_c-1} \alpha_{N_c-1}}, \end{aligned} \quad (13)$$

where  $f_1 \dots f_{N_c-1}$  and  $\alpha_1 \dots \alpha_{N_c-1}$  denote, respectively, the spin-isospin and color indices.  $\Gamma_{(TT_3 Y)(JJ_3 Y_R)}$  are matrices with the quantum numbers  $(TT_3 Y)(JJ_3 Y_R)$  for the corresponding baryon. For example, a singly heavy baryon  $\Sigma_c^+$  can be identified as the state with  $J = 1/2$ ,  $T = 1$ ,  $T_3 = 0$ , and  $Y = 2/3$ . The right hypercharge  $Y_R$  for singly heavy baryons is constrained by the number of the valence quarks. Note that  $Y_R = N_c/3$  for a light baryon, whereas  $Y_R = (N_c - 1)/3$  for a singly heavy baryon. The right hypercharge  $Y_R = 1$  with  $N_c = 3$  allows one to get the lowest-lying representations for the SU(3) baryons, i.e., the baryon octet (**8**) and decuplet (**10**) for the light baryons. On the other hand, we find the baryon antitriplet ( $\bar{\mathbf{3}}$ ), sextet (**6**), and so on [25,36].  $\psi_{f_k \alpha_k}(x)$  denotes the light-quark field, and  $\Psi_h(x)$  stands for the heavy-quark field. In

the limit of  $m_Q \rightarrow \infty$ , a singly heavy baryon satisfies the heavy-quark flavor symmetry. Then, the heavy-quark field can be written as

$$\Psi_h(x) = \exp(-im_Q v \cdot x) \tilde{\Psi}_h(x), \quad (14)$$

where  $\tilde{\Psi}_h(x)$  is a rescaled heavy-quark field almost on mass shell. It carries no information on the heavy-quark mass in the leading-order approximation in the heavy-quark expansion.  $v$  denotes the velocity of the heavy quark [29–31,41].

We can show explicitly that the normalization factor  $\mathcal{N}^*(\mathbf{p}') \mathcal{N}(\mathbf{p})$  correctly turns out to be  $2M_B$ . The normalization of the baryon state can be computed as

$$\begin{aligned} \langle B(p', J'_3) | B(p, J_3) \rangle &= \frac{1}{\mathcal{Z}_{\text{eff}}} \mathcal{N}^*(p') \mathcal{N}(p) \lim_{x_4 \rightarrow -\infty} \lim_{y_4 \rightarrow \infty} \exp(-iy_4 p'_4 + ix_4 p_4) \\ &\quad \times \int d^3x d^3y \exp(-i\mathbf{p}' \cdot \mathbf{y} + i\mathbf{p} \cdot \mathbf{x}) \int \mathcal{D}U \mathcal{D}\psi \mathcal{D}\psi^\dagger \mathcal{D}\tilde{\Psi}_h \mathcal{D}\tilde{\Psi}_h^\dagger J_B(y) \Psi_h(y) (-i\Psi_h^\dagger(x) \gamma_4) J_B^\dagger(x) \\ &\quad \times \exp \left[ \int d^4z \{ (\psi^\dagger(z))_\alpha^f (i\cancel{\partial} + iMU\gamma_5 + i\hat{m})_{fg} \psi^{g\alpha}(z) + \Psi_h^\dagger(z) v \cdot \partial \Psi_h(z) \} \right] \\ &= \frac{1}{\mathcal{Z}_{\text{eff}}} \mathcal{N}^*(p') \mathcal{N}(p) \lim_{x_4 \rightarrow -\infty} \lim_{y_4 \rightarrow \infty} \exp(-iy_4 p'_4 + ix_4 p_4) \\ &\quad \times \int d^3x d^3y \exp(-i\mathbf{p}' \cdot \mathbf{y} + i\mathbf{p} \cdot \mathbf{x}) \langle J_B(y) \Psi_h(y) (-i\Psi_h^\dagger(x) \gamma_4) J_B^\dagger(x) \rangle_0, \end{aligned} \quad (15)$$

where  $\mathcal{Z}_{\text{eff}}$  represents the low-energy effective QCD partition function defined as

$$\mathcal{Z}_{\text{eff}} = \int \mathcal{D}U \exp(-S_{\text{eff}}). \quad (16)$$

$S_{\text{eff}}$  is called the effective chiral action defined by

$$S_{\text{eff}} = -N_c \text{Tr} \ln [i\hat{\not{D}} + iMU^{\gamma_5} + i\hat{m}]. \quad (17)$$

$\langle \dots \rangle_0$  in Eq. (15) denotes the vacuum expectation value of the baryon correlation function.  $M$  represents the dynamical quark mass that arises from the spontaneous breakdown of chiral symmetry. The  $U^{\gamma_5}$  denotes the chiral field that is defined by

$$U^{\gamma_5}(z) = \frac{1 - \gamma_5}{2} U(z) + U^\dagger(z) \frac{1 + \gamma_5}{2} \quad (18)$$

with

$$U(z) = \exp[i\pi^a(z)\lambda^a], \quad (19)$$

where  $\pi^a(z)$  represents the pseudo-Nambu-Goldstone (pNG) fields and  $\lambda^a$  are the flavor Gell-Mann matrices.  $\hat{m}$  designates the mass matrix of current quarks  $\hat{m} = \text{diag}(m_u, m_d, m_s)$ . Note that we deal with the strange current quark mass  $m_s$  perturbatively. Thus, we will consider it when we make a zero-mode quantization for a collective baryon state. The propagators of a light quark in the  $\chi$ QSM [23] are given by

$$\begin{aligned} G(y, x) &= \langle y | \frac{1}{i\hat{\not{D}} + iMU^{\gamma_5} + i\hat{m}} (i\gamma_4) | x \rangle \\ &= \Theta(y_4 - x_4) \sum_{E_n > 0} e^{-E_n(y_4 - x_4)} \psi_n(\mathbf{y}) \psi_n^\dagger(\mathbf{x}) \\ &\quad - \Theta(x_4 - y_4) \sum_{E_n < 0} e^{-E_n(y_4 - x_4)} \psi_n(\mathbf{y}) \psi_n^\dagger(\mathbf{x}), \end{aligned} \quad (20)$$

where  $\Theta(y_4 - x_4)$  stands for the Heaviside step function. Here,  $\bar{m}$  represents the average mass of the up and down current quarks:  $\bar{m} = (m_u + m_d)/2$ .  $E_n$  is the energy eigenvalues of the single-quark state given by

$$H\psi_n(\mathbf{x}) = E_n\psi_n(\mathbf{x}), \quad (21)$$

where  $H$  denotes the one-body Dirac Hamiltonian in the presence of the pNG boson fields, which is defined by

$$H = \gamma_4 \gamma_i \partial_i + \gamma_4 M U^{\gamma_5} + \gamma_4 \bar{m} \mathbf{1}. \quad (22)$$

The heavy-quark propagator in the limit of  $m_Q \rightarrow \infty$  is expressed as

$$G_h(y, x) = \langle y | \frac{1}{\partial_4} | x \rangle = \Theta(y_4 - x_4) \delta^{(3)}(\mathbf{y} - \mathbf{x}). \quad (23)$$

Using these quark propagators and taking the limit of  $y_4 - x_4 = T \rightarrow \infty$ , we can derive the baryon correlation function  $\langle J_B(y) \Psi_h(y) (-i\Psi_h^\dagger(x) \gamma_4) J_B^\dagger(x) \rangle_0$  as follows [23,42]:

$$\begin{aligned} &\langle J_B(y) \Psi_h(y) (-i\Psi_h^\dagger(x) \gamma_4) J_B^\dagger(x) \rangle_0 \\ &\sim \exp[-\{(N_c - 1)E_{\text{val}} + E_{\text{sea}} + m_Q\}T] \\ &= \exp[-M_B T]. \end{aligned} \quad (24)$$

The result for the correlation function given in Eq. (24) is canceled with the term  $\exp(-iy_4 p'_4 + ix_4 p_4) = \exp[M_B T]$  in the large  $N_c$  limit, i.e.,  $-ip'_4 = -ip_4 = M_B = \mathcal{O}(N_c)$ . Thus, the normalization factor becomes  $\mathcal{N}^*(\mathbf{p}') \mathcal{N}(\mathbf{p}) = 2M_B$ . Using this normalization and Eq. (24), we are able to produce the classical mass of the singly heavy baryon correctly to be

$$M_B = (N_c - 1)E_{\text{val}} + E_{\text{sea}} + m_Q, \quad (25)$$

which was already defined in a previous work [26].

#### IV. EM TRANSITION FORM FACTORS FROM THE CHIRAL QUARK-SOLITON MODEL

In the present section, we will present here only the final expressions of the EM transition form factors, since detailed formalisms of how to derive the form factors of the SU(3) baryons can be found in previous works. For a detailed calculation, we refer to Refs. [43–45] (see also the review [42]). The EM current for the heavy quark given in the second term of Eq. (3) can be expressed in terms of the effective heavy-quark field [46]

$$\begin{aligned} &-i\Psi_h^\dagger(x) \gamma^\mu Q_h \Psi_h(x) \\ &= -i \exp(-im_Q v \cdot x) \tilde{\Psi}_h^\dagger(x) \left[ v_\mu + \frac{i}{2m_Q} (\tilde{\partial}_\mu - \bar{\partial}_\mu) \right. \\ &\quad \left. + \frac{1}{2m_Q} \sigma_{\mu\nu} (\tilde{\partial}_\mu + \bar{\partial}_\mu) \right] Q_h \tilde{\Psi}_h(x) \\ &\approx -i \exp(-im_Q v \cdot x) \tilde{\Psi}_h^\dagger(x) v_\mu Q_h \tilde{\Psi}_h(x). \end{aligned} \quad (26)$$

This indicates that the heavy quark does not contribute to the EM transition form factors of the singly heavy baryons. It only gives a constant contribution to their electric form factors, which yields the correct charges corresponding to the singly heavy baryon. Thus, we can simply consider the light-quark current to compute the matrix element of the EM current [44]

$$\begin{aligned} \langle B^*, p' | V^\mu(0) | B, p \rangle &= \frac{1}{\mathcal{Z}_{\text{eff}}} \lim_{T \rightarrow \infty} \exp \left[ -i(p'_4 + p_4) \frac{T}{2} \right] \int d^3x d^3y \exp(-i\mathbf{p}' \cdot \mathbf{y} + i\mathbf{p} \cdot \mathbf{x}) \int \mathcal{D}U \mathcal{D}\psi \mathcal{D}\psi^\dagger \\ &\quad \times J_{B^*}(\mathbf{y}, T/2) (-i\psi^\dagger(0)) \gamma_\mu \hat{Q} \psi(0) J_B^\dagger(\mathbf{x}, -T/2) \exp \left[ \int d^4z (\psi^\dagger(z))_\alpha^f (i\hat{\not{D}} + iMU^{\gamma_5} + i\hat{m})_{fg} \psi^{g\alpha}(z) \right]. \end{aligned} \quad (27)$$

Since we ignore the meson fluctuation, the integration over the pNG fields can be carried out easily. However, there are the rotational and translational zero modes that are not at all small, so we need to integrate exactly over these zero modes. This is known as the collective zero-mode quantization. For details about the zero-mode quantization in the SU(3)  $\chi$ QSM, we refer to Refs. [24,42].

Having taken into account the rotational  $1/N_c$  and linear  $m_s$  corrections, we obtain the magnetic dipole form factors  $G_{M1}^{B \rightarrow B^*}$  as

$$G_{M1}^{B \rightarrow B^*}(Q^2) = -c_\Delta \int d^3r \frac{6}{\sqrt{2}} j_1(|\mathbf{q}||\mathbf{r}|) \mathcal{G}_{M1}^{B \rightarrow B^*}(\mathbf{r}), \quad (28)$$

where the corresponding magnetic dipole densities  $\mathcal{G}_{M1}^{B \rightarrow B^*}(\mathbf{r})$  are defined as

$$\begin{aligned} \mathcal{G}_{M1}^{B \rightarrow B^*}(\mathbf{r}) = & \left( \mathcal{Q}_0(\mathbf{r}) + \frac{1}{I_1} \mathcal{Q}_1(\mathbf{r}) \right) \langle B^* | D_{Q3}^{(8)} | B \rangle - \frac{1}{\sqrt{3}} \frac{1}{I_1} \mathcal{X}_1(\mathbf{r}) \langle B^* | D_{Q8}^{(8)} J_3 | B \rangle - \frac{1}{I_2} \mathcal{X}_2(\mathbf{r}) \langle B^* | d_{pq3} D_{Qp}^{(8)} J_q | B \rangle \\ & - \frac{2}{3} m_s \left( \frac{K_1}{I_1} \mathcal{X}_1(\mathbf{r}) - \mathcal{M}_1(\mathbf{r}) \right) \langle B^* | D_{83}^{(8)} D_{Q8}^{(8)} | B \rangle - \frac{2}{\sqrt{3}} m_s \left( \frac{K_2}{I_2} \mathcal{X}_2(\mathbf{r}) - \mathcal{M}_2(\mathbf{r}) \right) \langle B^* | d_{pq3} D_{8p}^{(8)} D_{Qq}^{(8)} | B \rangle \\ & - \frac{2}{3} m_s \mathcal{M}_0(\mathbf{r}) \langle B^* | D_{Q3}^{(8)} | B \rangle + \frac{2}{3} m_s \mathcal{M}_0(\mathbf{r}) \langle B^* | D_{88}^{(8)} D_{Q3}^{(8)} | B \rangle. \end{aligned} \quad (29)$$

The explicit expressions for the densities  $\mathcal{Q}_i$ ,  $\mathcal{X}$ , and  $\mathcal{M}_i$  can be found in Appendix A. The  $\langle B^* | \dots | B \rangle$  stands for the matrix elements of collective operators [35], of which the explicit values are found in Appendix B.  $I_i$  and  $K_i$  stand for the moments and anomalous moments of inertia [42]. The expression for the electric quadrupole form factors is given as

$$G_{E2}^{B \rightarrow B^*}(Q^2) = c_\Delta \int d^3r \sqrt{\frac{10}{9}} \frac{\omega_q}{|\mathbf{q}|} \left( \frac{\partial}{\partial r} r j_2(|\mathbf{q}||\mathbf{r}|) \right) \mathcal{G}_{E2}^{B \rightarrow B^*}(\mathbf{r}), \quad (30)$$

with the electric quadrupole densities  $\mathcal{G}_{E2}^{B \rightarrow B^*}(\mathbf{r})$ ,

$$\begin{aligned} \mathcal{G}_{E2}^{B \rightarrow B^*}(\mathbf{r}) = & -\frac{2}{I_1} \mathcal{I}_{1E2}(\mathbf{r}) (3 \langle B^* | D_{Q3}^{(8)} J_3 | B \rangle - \langle B^* | D_{Qi}^{(8)} J_i | B \rangle) \\ & - \frac{4}{\sqrt{3}} m_s \left( \frac{K_1}{I_1} \mathcal{I}_{1E2}(\mathbf{r}) - \mathcal{K}_{1E2}(\mathbf{r}) \right) (3 \langle B^* | D_{83}^{(8)} D_{Q3}^{(8)} | B \rangle - \langle B^* | D_{8i}^{(8)} D_{Qi}^{(8)} | B \rangle). \end{aligned} \quad (31)$$

The explicit expressions for  $\mathcal{I}_{1E2}(\mathbf{r})$  and  $\mathcal{K}_{1E2}(\mathbf{r})$  can be found in Appendix A. The Coulomb quadrupole form factor  $G_{C2}^{B \rightarrow B^*}$  is written as

$$G_{C2}^{B \rightarrow B^*}(Q^2) = c_\Delta \sqrt{40} \int d^3r \frac{M_{B^*}}{|\mathbf{q}|} j_2(|\mathbf{q}||\mathbf{r}|) \mathcal{G}_{C2}^{B \rightarrow B^*}(\mathbf{r}), \quad (32)$$

where  $\mathcal{G}_{C2}^{B \rightarrow B^*}(\mathbf{r})$  is simply the same as  $\mathcal{G}_{E2}^{B \rightarrow B^*}(\mathbf{r})$ . Note that for the E2 and C2 form factors, the leading contributions in the large  $N_c$  expansion vanish, so that the rotational  $1/N_c$  corrections take over the role of the leading-order contributions. Note that the present model satisfies a general scheme of large- $N_c$  QCD [47].

To scrutinize each contribution, it is more convenient to decompose the densities into three different terms:

$$\begin{aligned} \mathcal{G}_{(M1,E2,C2)}^{B \rightarrow B^*}(\mathbf{r}) = & \mathcal{G}_{(M1,E2,C2)}^{B \rightarrow B^*(0)}(\mathbf{r}) + \mathcal{G}_{(M1,E2,C2)}^{B \rightarrow B^*(\text{op})}(\mathbf{r}) \\ & + \mathcal{G}_{(M1,E2,C2)}^{B \rightarrow B^*(\text{wf})}(\mathbf{r}). \end{aligned} \quad (33)$$

The first term represents the SU(3) symmetric terms including both the leading and rotational  $1/N_c$  contributions, the second one denotes the linear  $m_s$  corrections arising from the current-quark mass term of the effective chiral action, and the last terms come from the collective baryon wave functions. When the effects of the flavor SU(3) symmetry breaking are considered, a collective baryon wave function is not any longer in a pure state but becomes a state mixed with higher representations. Thus, there are two different terms that provide the effects of flavor SU(3) symmetry breaking. The explicit expressions of these three terms for the M1 form factors are then given as

$$\mathcal{G}_{M1}^{\bar{3}_{1/2} \rightarrow 6_{3/2}^{(0)}}(\mathbf{r}) = \frac{1}{4\sqrt{3}} \mathcal{Q}_{B \rightarrow B^*} \left( \mathcal{Q}_0(\mathbf{r}) + \frac{1}{I_1} \mathcal{Q}_1(\mathbf{r}) + \frac{1}{2I_2} \mathcal{X}_2(\mathbf{r}) \right), \quad (34)$$

$$\begin{aligned} \mathcal{G}_{M1}^{\bar{3}_{1/2} \rightarrow \mathbf{6}_{3/2}(\text{op})}(\mathbf{r}) = & -\frac{m_s}{60\sqrt{3}} \begin{pmatrix} \mathcal{Q}_{\Lambda_c \rightarrow \Sigma_c^*} \\ -4\mathcal{Q}_{\Xi_c \rightarrow \Xi_c^*} + 3 \end{pmatrix} \left( \frac{K_1}{I_1} \mathcal{X}_1(\mathbf{r}) - \mathcal{M}_1(\mathbf{r}) \right) \\ & - \frac{m_s}{10\sqrt{3}} \begin{pmatrix} \mathcal{Q}_{\Lambda_c \rightarrow \Sigma_c^*} \\ -\mathcal{Q}_{\Xi_c \rightarrow \Xi_c^*} + 2 \end{pmatrix} \left( \frac{K_2}{I_2} \mathcal{X}_2(\mathbf{r}) - \mathcal{M}_2(\mathbf{r}) \right) + \frac{m_s}{60\sqrt{3}} \begin{pmatrix} -7\mathcal{Q}_{\Lambda_c \rightarrow \Sigma_c^*} \\ \mathcal{Q}_{\Xi_c \rightarrow \Xi_c^*} + 1 \end{pmatrix} \mathcal{M}_0(\mathbf{r}), \end{aligned} \quad (35)$$

$$\begin{aligned} \mathcal{G}_{M1}^{\bar{3}_{1/2} \rightarrow \mathbf{6}_{3/2}(\text{wf})}(\mathbf{r}) = & \frac{q\sqrt{15}}{40\sqrt{6}} \begin{pmatrix} 4\mathcal{Q}_{\Lambda_c \rightarrow \Sigma_c^*} \\ -\mathcal{Q}_{\Xi_c \rightarrow \Xi_c^*} + 2 \end{pmatrix} \left( \mathcal{Q}_0(\mathbf{r}) + \frac{1}{I_1} \mathcal{Q}_1(\mathbf{r}) - \frac{1}{2} \frac{1}{I_2} \mathcal{X}_2(\mathbf{r}) \right) \\ & - \frac{p\sqrt{15}}{240} \begin{pmatrix} 2\mathcal{Q}_{\Lambda_c \rightarrow \Sigma_c^*} \\ -5\mathcal{Q}_{\Xi_c \rightarrow \Xi_c^*} + 4 \end{pmatrix} \left( \mathcal{Q}_0(\mathbf{r}) + \frac{1}{I_1} \mathcal{Q}_1(\mathbf{r}) + \frac{3}{2} \frac{1}{I_2} \mathcal{X}_2(\mathbf{r}) \right), \end{aligned} \quad (36)$$

in the basis of the  $[\Lambda_c \rightarrow \Sigma_c^*, \Xi_c \rightarrow \Xi_c^*]$  for  $\bar{3}_{1/2} \rightarrow \mathbf{6}_{3/2}$ , and

$$\mathcal{G}_{M1}^{\mathbf{6}_{1/2} \rightarrow \mathbf{6}_{3/2}(0)}(\mathbf{r}) = \frac{1}{30\sqrt{2}} (3\mathcal{Q}_{B \rightarrow B^*} - 2) \left( \mathcal{Q}_0(\mathbf{r}) + \frac{1}{I_1} \mathcal{Q}_1(\mathbf{r}) + \frac{1}{3} \frac{1}{I_1} \mathcal{X}_1(\mathbf{r}) + \frac{1}{2} \frac{1}{I_2} \mathcal{X}_2(\mathbf{r}) \right), \quad (37)$$

$$\begin{aligned} \mathcal{G}_{M1}^{\mathbf{6}_{1/2} \rightarrow \mathbf{6}_{3/2}(\text{op})}(\mathbf{r}) = & -\frac{m_s}{270\sqrt{2}} \begin{pmatrix} 4\mathcal{Q}_{\Sigma_c \rightarrow \Sigma_c^*} - 5 \\ 2\mathcal{Q}_{\Xi_c' \rightarrow \Xi_c^*} - 1 \\ 2\mathcal{Q}_{\Omega_c \rightarrow \Omega_c^*} + 3 \end{pmatrix} \left( \frac{K_1}{I_1} \mathcal{X}_1(\mathbf{r}) - \mathcal{M}_1(\mathbf{r}) \right) \\ & - \frac{m_s}{135\sqrt{2}} \begin{pmatrix} 5\mathcal{Q}_{\Sigma_c \rightarrow \Sigma_c^*} + 7 \\ 7\mathcal{Q}_{\Xi_c' \rightarrow \Xi_c^*} - 2 \\ \mathcal{Q}_{\Omega_c \rightarrow \Omega_c^*} + 3 \end{pmatrix} \left( \frac{K_2}{I_2} \mathcal{X}_2(\mathbf{r}) - \mathcal{M}_2(\mathbf{r}) \right) + \frac{m_s}{270\sqrt{2}} \begin{pmatrix} -14\mathcal{Q}_{\Sigma_c \rightarrow \Sigma_c^*} + 7 \\ -16\mathcal{Q}_{\Xi_c' \rightarrow \Xi_c^*} + 11 \\ -16\mathcal{Q}_{\Omega_c \rightarrow \Omega_c^*} + 15 \end{pmatrix} \mathcal{M}_0(\mathbf{r}), \end{aligned} \quad (38)$$

$$\begin{aligned} \mathcal{G}_{M1}^{\mathbf{6}_{1/2} \rightarrow \mathbf{6}_{3/2}(\text{wf})}(\mathbf{r}) = & \frac{q\sqrt{15}}{180} \begin{pmatrix} 4\mathcal{Q}_{\Sigma_c \rightarrow \Sigma_c^*} - 8 \\ \mathcal{Q}_{\Xi_c' \rightarrow \Xi_c^*} - 4 \\ 0 \end{pmatrix} \left( \mathcal{Q}_0(\mathbf{r}) + \frac{1}{I_1} \mathcal{Q}_1(\mathbf{r}) - \frac{1}{I_1} \mathcal{X}_1(\mathbf{r}) - \frac{1}{2} \frac{1}{I_2} \mathcal{X}_2(\mathbf{r}) \right) \\ & - \frac{q\sqrt{24}}{180\sqrt{5}} \begin{pmatrix} \mathcal{Q}_{\Sigma_c \rightarrow \Sigma_c^*} + 1 \\ 2\mathcal{Q}_{\Xi_c' \rightarrow \Xi_c^*} + 4 \\ 3\mathcal{Q}_{\Omega_c \rightarrow \Omega_c^*} + 6 \end{pmatrix} \left( \mathcal{Q}_0(\mathbf{r}) + \frac{1}{I_1} \mathcal{Q}_1(\mathbf{r}) - \frac{2}{I_1} \mathcal{X}_1(\mathbf{r}) - \frac{2}{I_2} \mathcal{X}_2(\mathbf{r}) \right), \end{aligned} \quad (39)$$

in the basis of the  $[\Sigma_c \rightarrow \Sigma_c^*, \Xi_c' \rightarrow \Xi_c^*, \Omega_c \rightarrow \Omega_c^*]$  for  $\mathbf{6}_{1/2} \rightarrow \mathbf{6}_{3/2}$ . Similarly, the densities for the E2 form factors are written by

$$\mathcal{G}_{E2}^{\mathbf{6}_{1/2} \rightarrow \mathbf{6}_{3/2}(0)}(\mathbf{r}) = -\frac{1}{5\sqrt{2}} (3\mathcal{Q}_{B \rightarrow B^*} - 2) \frac{1}{I_1} \mathcal{I}_{1E2}, \quad (40)$$

$$\mathcal{G}_{E2}^{\mathbf{6}_{1/2} \rightarrow \mathbf{6}_{3/2}(\text{op})}(\mathbf{r}) = -\frac{8m_s}{135\sqrt{2}} \begin{pmatrix} -2\mathcal{Q}_{\Sigma_c \rightarrow \Sigma_c^*} + 1 \\ 8\mathcal{Q}_{\Xi_c' \rightarrow \Xi_c^*} - 1 \\ -8\mathcal{Q}_{\Omega_c \rightarrow \Omega_c^*} + 3 \end{pmatrix} \left( \frac{K_1}{I_1} \mathcal{I}_{1E2}(\mathbf{r}) - \mathcal{K}_{1E2}(\mathbf{r}) \right), \quad (41)$$

$$\mathcal{G}_{E2}^{\mathbf{6}_{1/2} \rightarrow \mathbf{6}_{3/2}(\text{wf})}(\mathbf{r}) = -\frac{1}{30} \left[ q\sqrt{15} \begin{pmatrix} 4\mathcal{Q}_{\Sigma_c \rightarrow \Sigma_c^*} - 8 \\ 5\mathcal{Q}_{\Xi_c' \rightarrow \Xi_c^*} - 4 \\ 0 \end{pmatrix} - \frac{q\sqrt{24}}{\sqrt{5}} \begin{pmatrix} \mathcal{Q}_{\Sigma_c \rightarrow \Sigma_c^*} + 1 \\ 2\mathcal{Q}_{\Xi_c' \rightarrow \Xi_c^*} + 4 \\ 3\mathcal{Q}_{\Omega_c \rightarrow \Omega_c^*} + 6 \end{pmatrix} \right] \frac{1}{I_1} \mathcal{I}_{1E2}(\mathbf{r}), \quad (42)$$

in the basis of the  $[\Sigma_c \rightarrow \Sigma_c^*, \Xi_c' \rightarrow \Xi_c^*, \Omega_c \rightarrow \Omega_c^*]$  for  $\mathbf{6}_{1/2} \rightarrow \mathbf{6}_{3/2}$ .  $\mathcal{Q}_{B \rightarrow B^*}$  stand for the charges of the corresponding heavy baryons. Note that the E2 and C2 transition from factors  $[\bar{3}_{1/2}(J=0) \rightarrow \mathbf{6}_{3/2}(J=1)]$  are forbidden within this model.

## V. RESULTS AND DISCUSSION

### A. Comparison with the lattice data

Since we use exactly the same set of the model parameters as in Refs. [26,37,38], we proceed to present the numerical results and discuss them. To compare the present results with those from lattice QCD [20], we need to employ the values of the unphysical pion mass. We refer to Ref. [39] for details. In the left and right panels of Fig. 1, we draw, respectively, the results for the M1 and E2 transition form factors with the pion mass varied from the chiral limit ( $m_\pi = 0$ ) to  $m_\pi = 550$  MeV. We find that when the larger value of the pion mass is used the results for both the M1 and E2 form factors fall off more slowly, as  $Q^2$  increases. This feature is already known from the results for the EM form factors of both the light and singly heavy baryons [37–39,44]. There are only two lattice data at  $Q^2 = 0$  and  $Q^2 = 0.2$  GeV<sup>2</sup>, and they indicate that the lattice data on the M1 transition form factor of the  $\Omega_c^0 \gamma \rightarrow \Omega_c^{*0}$  process falls off rather slowly, compared to the present results with the corresponding value of the pion mass, i.e.,  $m_\pi = 156$  MeV. As shown in the left panel of Fig. 1, the present results are overestimated approximately by 50%. Considering the fact that the lattice data on the  $\Omega_c^0 \rightarrow \Omega_c^{*0}$  E2 transition form factor show large numerical uncertainties, we are not able to draw any definitive conclusions from the comparison with the lattice data. Actually, the lattice data on the E2 form factors of  $\Omega_c^{*0}$  contain similar uncertainties as shown in Ref. [48]. We anticipate future experimental and lattice data, which will allow one to make a quantitative comparison.

It is also interesting to see that the magnitude of the E2 form factor of the  $\Omega_c^{*0} \rightarrow \Omega_c$  transition increases drastically as  $Q^2$  gets closer to zero. This is in line with what was found in Ref. [9], where the radiative decay  $\Sigma_c^* \rightarrow \Lambda_c \gamma$  was examined. This indicates that the effects of the vacuum

polarization or the sea quarks become dominant over those of the valence quarks as  $Q^2$  decreases. We will later discuss each contribution of the valence and sea quarks to the E2 form factors in detail.

It is of great importance to know the magnetic dipole transition form factors of the baryon sextet with spin 3/2, since they provide essential information on their radiative decays. As expressed in Eq. (11), the values of the M1 and E2 transition form factors at  $Q^2 = 0$  will determine the decay rates of the radiative decays of the baryon sextet with spin 3/2. However, since the values of the E2 transition form factors are known to be rather small in the case of the baryon decuplet, we expect that they would be also small in the case of the baryon sextet with spin 3/2. As will be shown later, the magnitudes of the E2 transition form factors are indeed very small, compared with those of the M1 transition form factors.

### B. Valence- and sea-quark contributions

In Fig. 2, we show the results for the M1 form factors of the EM transitions from the baryon antitriplet to the baryon sextet with spin 3/2, drawing separately the valence- and sea-quark contributions. On the other hand, Fig. 3 depicts the results for those from the baryon sextet with spin 1/2 to the baryon sextet with spin 3/2, again with the valence- and sea-quark contributions separated. In general, the valence-quark contributions dominate over those of the sea quarks. In the case of the radiative excitation  $\Xi_c^0 \gamma \rightarrow \Xi_c^{*0}$ , the effect of the sea quarks is negligibly small. Note that the magnitude of this M1 form factor is approximately more than ten times smaller, compared with those for the  $\Lambda_c^+ \gamma \rightarrow \Sigma_c^{*+}$  and  $\Xi_c^+ \gamma \rightarrow \Xi_c^{*+}$  excitations. This is due to the  $U$ -spin symmetry, which will be discussed later. Comparing the results in Fig. 2 with those in Fig. 3, we find that the M1 excitations for the baryon antitriplet are larger than those for the baryon sextet except for the  $\Xi_c^0 \gamma \rightarrow \Xi_c^{*0}$  excitation.

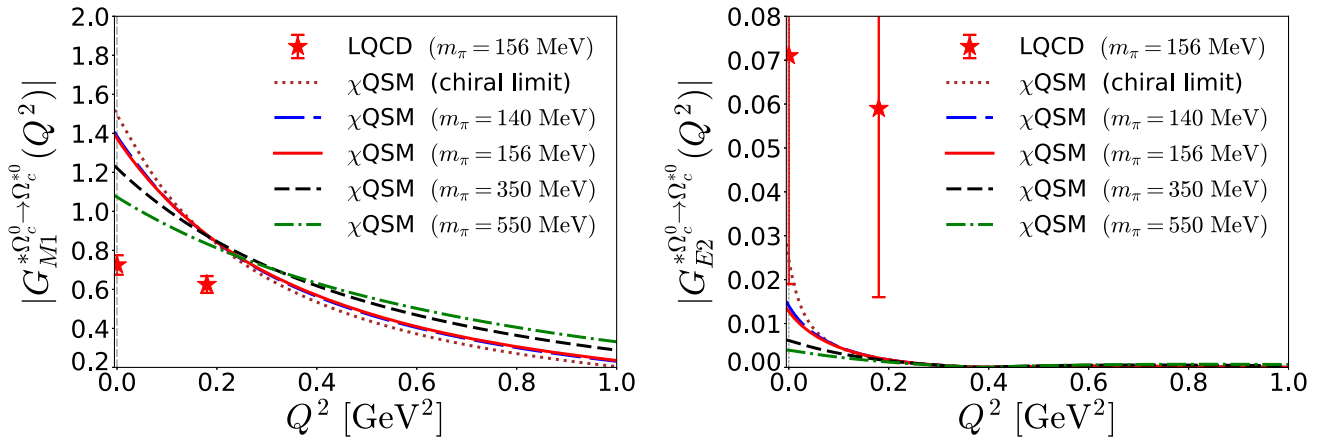


FIG. 1. Numerical results for the magnetic dipole and electric quadrupole transition form factors of the  $\Omega_c \gamma \rightarrow \Omega_c^*$  transition with the pion mass varied from 0 to 550 MeV, drawn, respectively, in the left and right panels. The results are compared with the lattice data taken from Ref. [20].

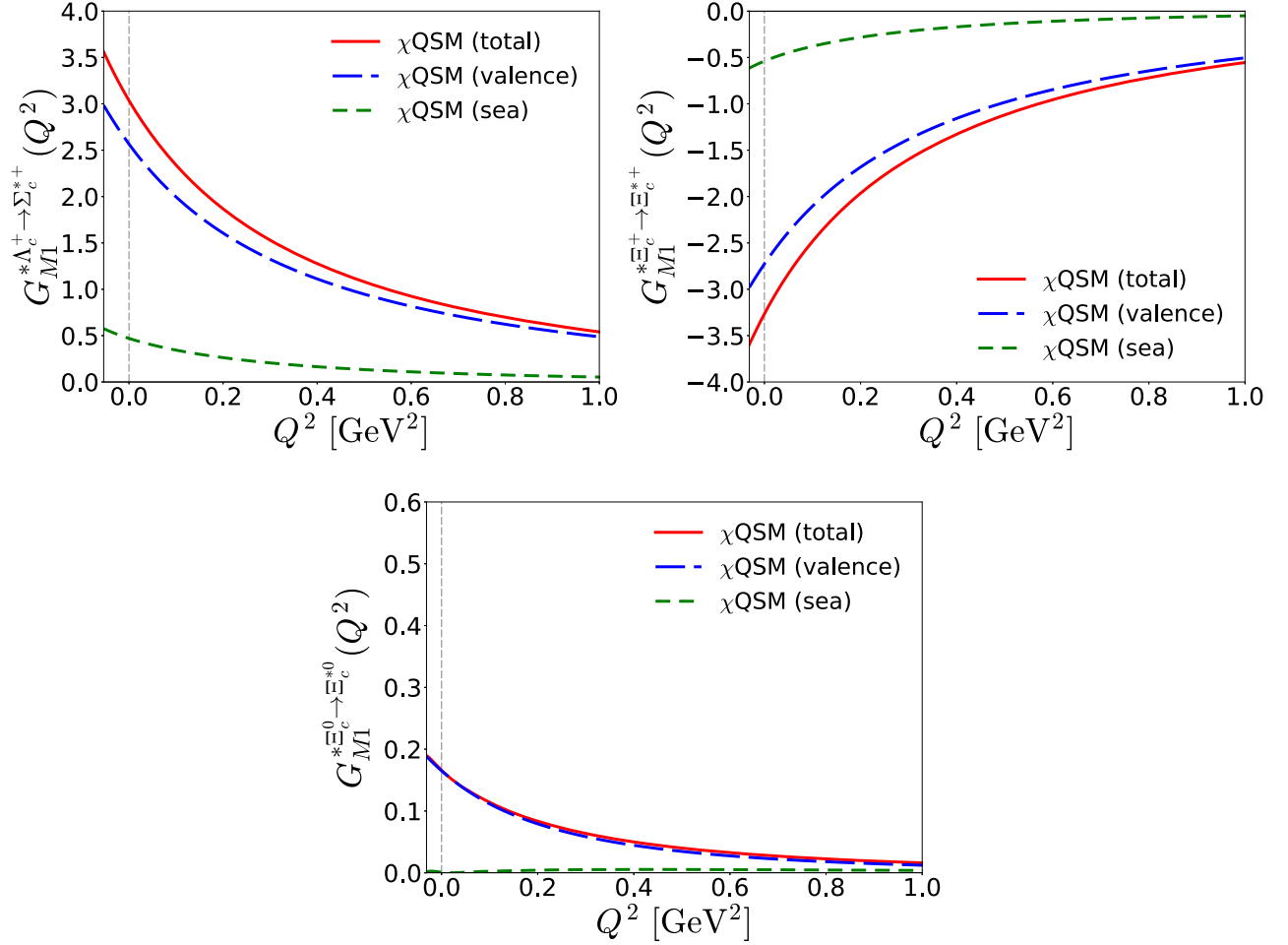


FIG. 2. Results for the magnetic dipole transition form factors from the baryon antitriplet to the baryon sextet with spin 3/2, with the valence- and sea-quark contributions separated. The dashed and short-dashed curves draw the valence- and sea-quark contributions, respectively. The solid ones depict the total results.

While this can be understood by comparing Eq. (34) with Eq. (37), the physical interpretation of these results is originated from the spin configuration of the light valence quarks inside heavy baryons. The spins of the light valence quarks for the baryon antitriplet are in the spin-singlet state ( $S_L = 0$ ), whereas those for the baryon sextet are in the spin-triplet state ( $S_L = 1$ ). The M1 transitions occur more likely due to the spin flip of the light valence quarks based on the naive quark model. Thus, the M1 form factors for the radiative excitations from the baryon antitriplet to the baryon sextet with spin 3/2 turn out naturally larger than those from the baryon sextet with spin 1/2 to the baryon sextet with spin 3/2. On the other hand, the sea-quark contribution arises from the polarized Dirac continuum due to the presence of the  $N_c - 1$  valence quarks. This can also be interpreted as the contributions of the pion clouds with spin zero in a traditional term. This means that those of the pion clouds are suppressed for the M1 transitions.

When it comes to the E2 transitions, the situation is the other way around. The E2 transitions are forbidden

between the different spin states. Thus, we have only the finite results for the E2 form factors for the EM transitions between the baryon sextet with spin 1/2 and with spin 3/2, as shown in Fig. 4. The sea-quark contributions to the E2 form factors are remarkably sizable, which was already shown in those of the baryon decuplet [43,44]. In the case of the  $\Xi_c^0 \rightarrow \Xi_c^{*0}$  and  $\Omega_c^0 \rightarrow \Omega_c^{*0}$  EM transitions, the sea-quark contributions dominate over those of the valence quarks, in particular, in the smaller  $Q^2$  region. This implies that the effects of the pion clouds play a significant role in describing the E2 form factors. Knowing the fact that the E2 transition form factors reveal how a baryon with spin 3/2 is deformed, the outer part of the charge distribution governs the E2 form factors. As shown in Refs. [45,49], the sea-quark part constructs the outer place of the charge and mechanical distributions in a baryon, whereas the valence-quark part is responsible for the inner part of these distributions. In this sense, it is natural that the sea-quark contributions contribute significantly to the E2 transition form factors in the smaller  $Q^2$  region. Note that

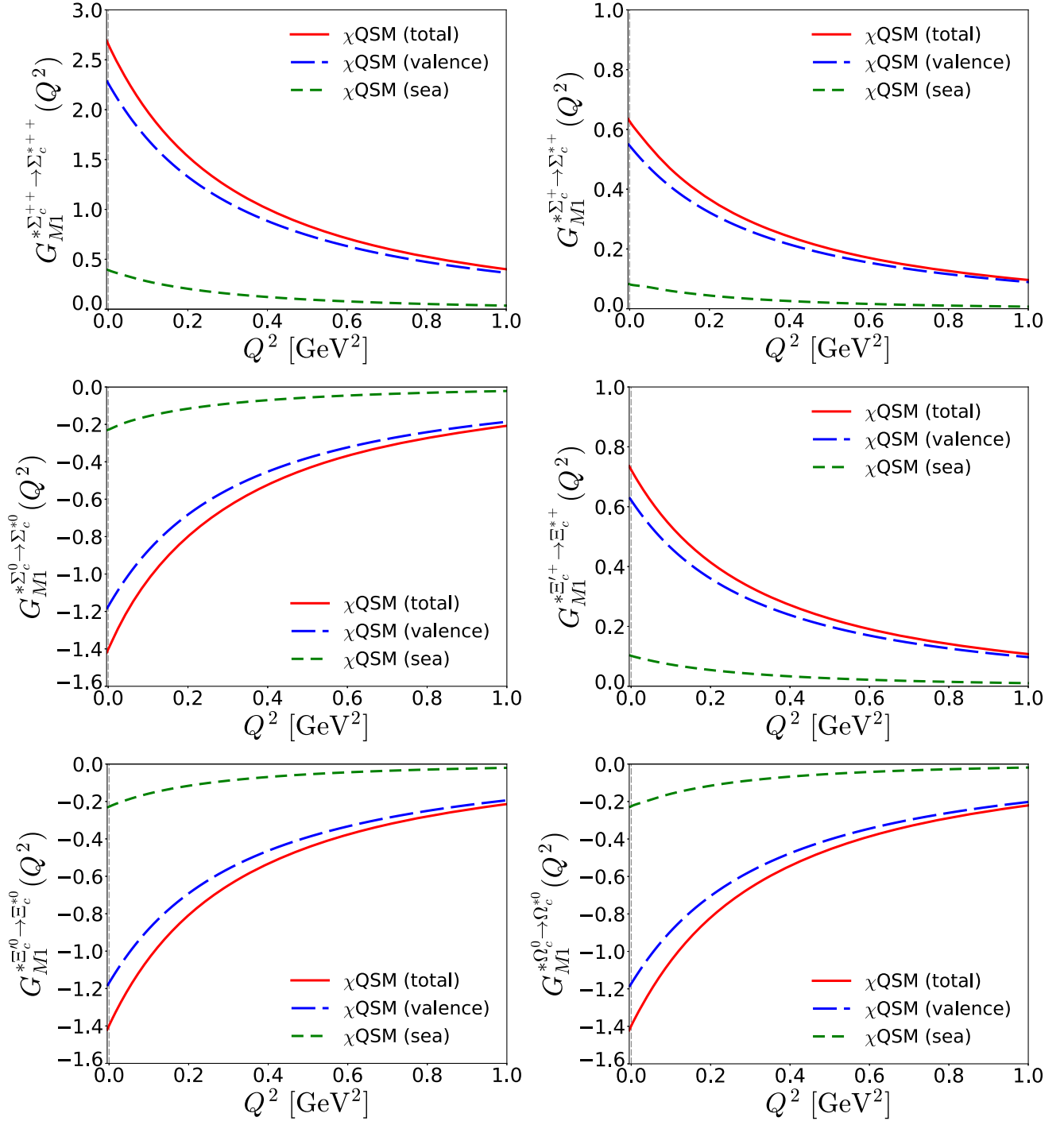


FIG. 3. Results for the magnetic dipole transition form factors from the baryon sextet with spin 1/2 to the baryon sextet with spin 3/2, with the valence- and sea-quark contributions separated. The notations are the same as in Fig. 2.

as  $Q^2$  increases the sea-quark contributions fall off much faster than those of the valence quarks, which is also understandable.

The magnitudes of the E2 transition form factors of a baryon are in general much smaller than those of the M1 transition form factors. The leading contribution to the E2 form factors vanishes within the  $\chi$ QSM, so the

rotational  $1/N_c$  correction takes the place of the leading contribution as shown in Eq. (40). This indicates that the magnitudes of the E2 form factors should be smaller than those of the M1 ones. Moreover, the E2 form factors are suppressed by the mass of a decaying baryon. Considering the fact that the mass of a singly heavy baryon is much larger than those of the baryon decuplet, one can expect

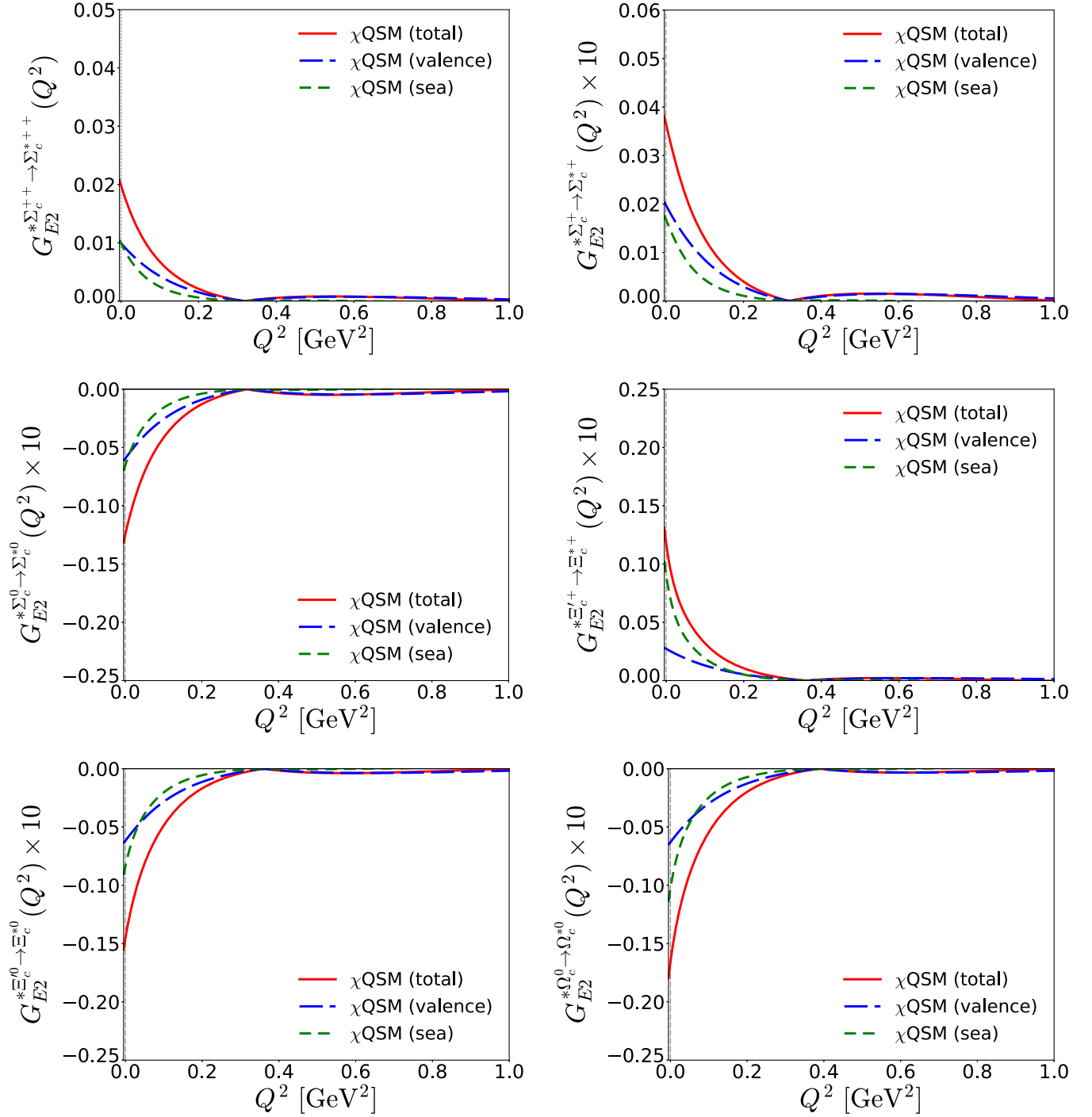


FIG. 4. Results for the electric quadrupole transition form factors from the baryon sextet with spin 1/2 to the baryon sextet with spin 3/2, with the valence- and sea-quark contributions separated. The notations are the same as in Fig. 2.

that the E2 transition form factors of the baryon sextet would turn out to be much smaller than those of the baryon decuplet. In addition, the matrix elements of the SU(3) Wigner  $D$  functions for the baryon sextet are smaller than those for the baryon decuplet. Thus, the magnitudes of the E2 transition form factors for the baryon sextet become approximately five to ten times

smaller than those for the baryon decuplet. Figure 5 presents the numerical results for the Coulomb quadrupole form factors from the baryon sextet with spin 1/2 to that with spin 3/2. The main conclusion is the same as in the case of the E2 transition form factors. The sea-quark contributions are again dominant over those of the valence quarks in the smaller  $Q^2$  region.

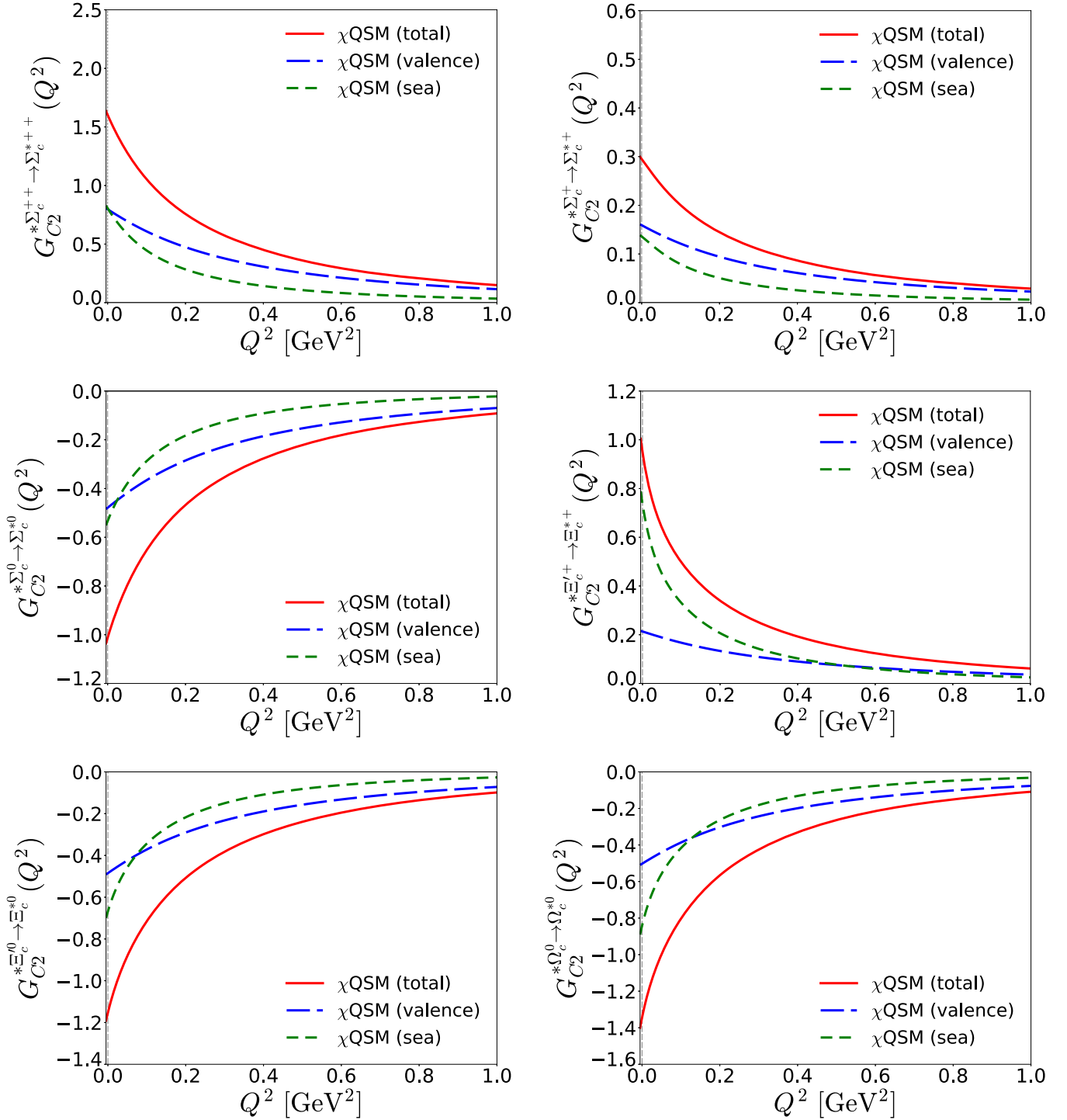


FIG. 5. Results for the Coulomb quadrupole transition form factors from the baryon sextet with spin 1/2 to the baryon sextet with spin 3/2, with the valence- and sea-quark contributions separated. The notations are the same as in Fig. 2.

### C. Effects of explicit breaking of flavor SU(3) symmetry

In Fig. 6, we examine the effects of flavor SU(3) symmetry breaking on the M1 transition form factors. While the linear  $m_s$  corrections are very small to the  $\Lambda_c^+ \rightarrow \Sigma_c^{*+}$  and  $\Xi_c^+ \rightarrow \Xi_c^{*+}$  magnetic transitions, they become the

leading contributions to the  $\Xi_c^0 \rightarrow \Xi_c^{*0}$ . The reason is clear as mentioned previously. The  $U$ -spin symmetry forbids the neutral EM transition from  $\Xi_c^0 \rightarrow \Xi_c^{*0}$ . As shown in Eq. (34), the SU(3) symmetric leading contributions are proportional to the charge of the singly heavy baryons involved in the transition due to the  $U$ -spin symmetry. Note

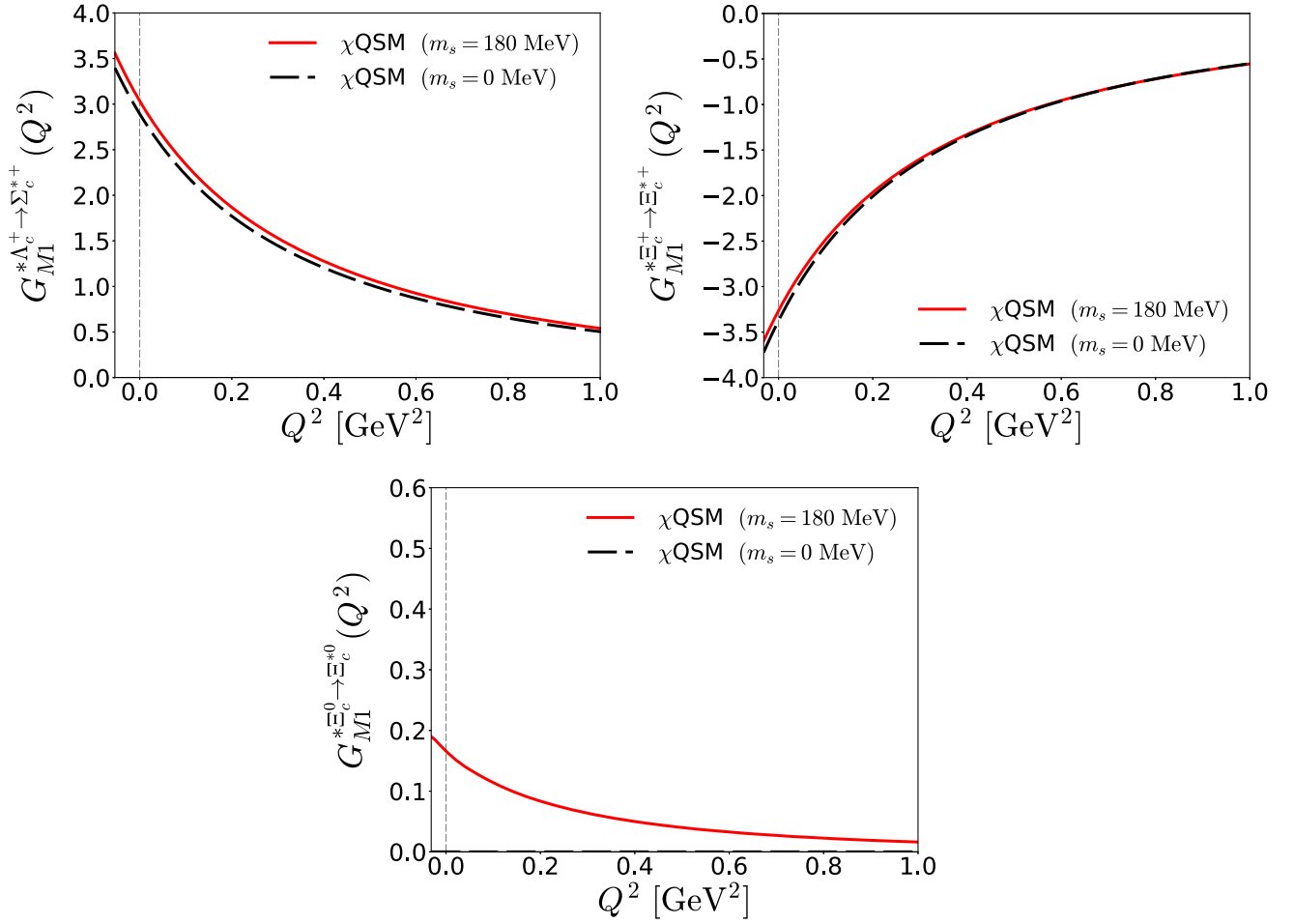


FIG. 6. Results for the magnetic dipole transition form factors from the baryon antitriplet to the baryon sextet with spin 3/2. The dashed curves draw the results in flavor SU(3) symmetry, whereas the solid ones depict those with flavor SU(3) symmetry breaking taken into account.

that  $\Xi_c^0$  belongs to the  $U$ -spin singlet, while  $\Xi_c^{*0}$  is the  $U$ -spin triplet. Only when  $m_s \neq m_{u,d}$ , it allows the  $\Xi_c^0 \rightarrow \Xi_c^{*0}$  transition mode. As a result, the magnitude of the  $\Xi_c^0 \rightarrow \Xi_c^{*0}$  M1 form factor is tiny, compared to those of the other M1 transition form factors. In Fig. 7, we depict the results for the M1 transition form factors from the baryon sextet with spin 1/2 to the baryon sextet with spin 3/2 with the linear  $m_s$  considered. The effects of the flavor SU(3) symmetry breaking are again negligibly small. It is interesting to compare these results with those for the M1 form factors of the baryon decuplet presented in Ref. [50]. While the linear  $m_s$  corrections are also very small in the case of the M1 transition form factors for the baryon decuplet, they turn out to be much smaller for the baryon sextet than for the decuplet. In the case of the E2 transition form factors, the linear  $m_s$  corrections are sizable for the  $\Sigma_c^+ \rightarrow \Sigma_c^{*+}$  and  $\Xi_c^+ \rightarrow \Xi_c^{*+}$  E2 excitations as shown in Fig. 8. It is also interesting to see that the linear  $m_s$  corrections suppress the E2 transition form factors for the  $\Sigma_c^+ \rightarrow \Sigma_c^{*+}$  excitation. These can be understood by examining Eqs. (41) and (42).

In Fig. 9, we draw the numerical results for the C2 transition form factors from the baryon sextet with spin 1/2 to that with spin 3/2. Knowing that the densities for them are the same as those for the E2 transition form factors, we can understand the sizable effects of the linear  $m_s$  on the  $\Sigma_c^+ \rightarrow \Sigma_c^{*+}$  and  $\Xi_c^+ \rightarrow \Xi_c^{*+}$  transitions.

#### D. Decay widths of the radiative decay for the baryon sextet with spin 3/2

In Table I, we list the results for the widths of the radiative decays from the baryon sextet with spin 3/2 to the baryon antitriplet in the first three lines and to the baryon sextet with spin 1/2 in the next lines. As written in Eq. (11), the decay width for the  $B_{3/2}^* \rightarrow B_{1/2}\gamma$  is proportional to  $|G_{M1}^*|^2 + 3|G_{E2}^*|^2$ . Since we have already shown that the values of  $G_{E2}^*$  are much smaller than those of  $G_{M1}^*$ , the decay widths are approximately proportional to  $|G_{M1}^*|^2$ . The results Results for the radiative decay widths of  $B\gamma \rightarrow B^*$ , which are listed in Table I, indicate that the

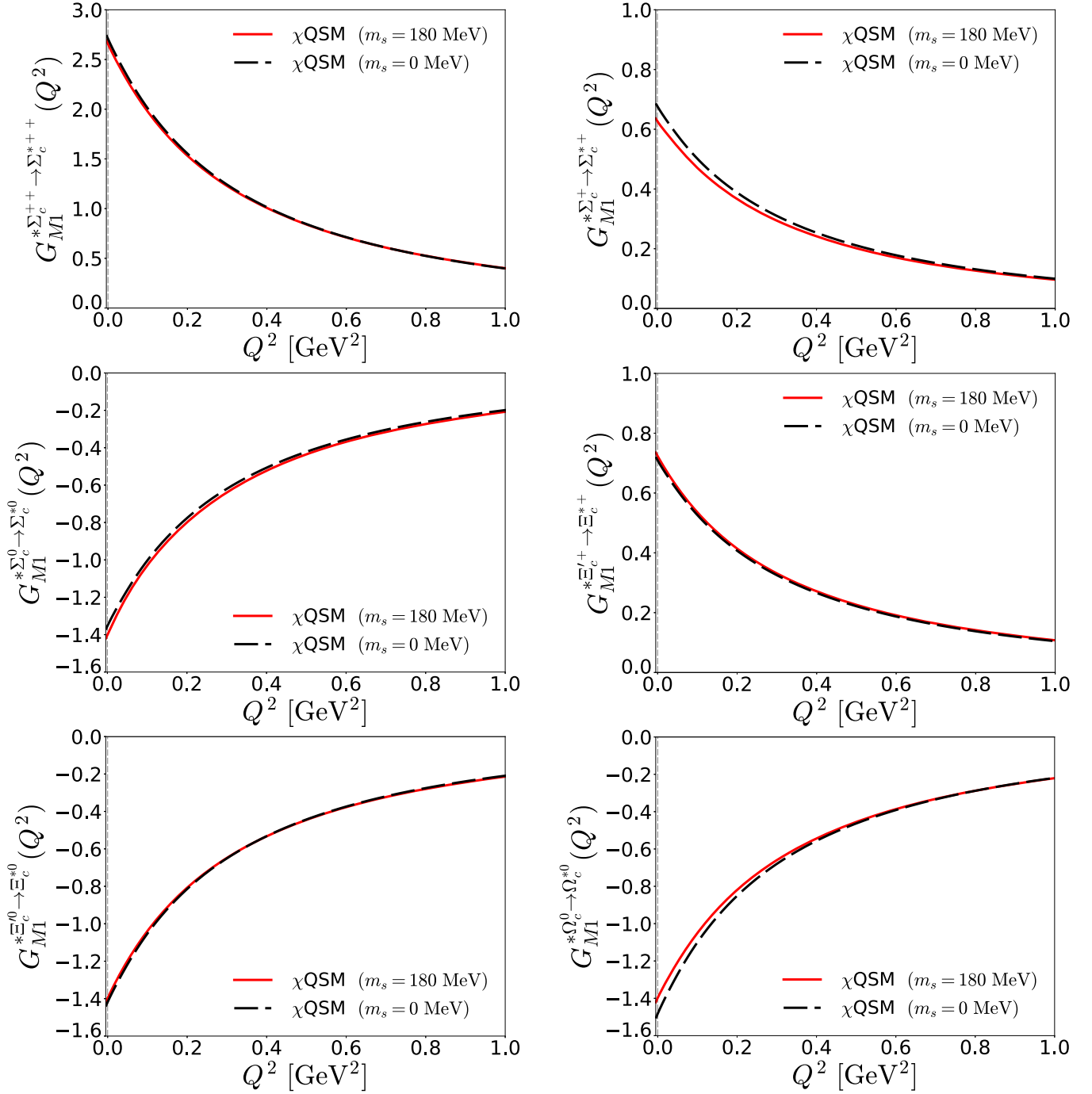


FIG. 7. Results for the magnetic dipole transition form factors from the baryon sextet with spin 1/2 to the baryon sextet with spin 3/2. The notations are the same as in Fig. 6.

baryons in the sextet are more likely to decay into those in the antitriplet. As explained previously, the spin state of the decaying baryon is flipped in the M1 transition. This explains why the decay rates from the baryon sextet with spin 3/2 to the baryon antitriplet are much larger than the  $\mathbf{6}_{3/2} \rightarrow \mathbf{6}_{1/2}\gamma$  decays. As we have already seen from the results for the form factors, the effects of the flavor SU(3) symmetry are rather small. The fourth column lists the

results from the chiral quark-soliton model in a model-independent approach [35] where all dynamical variables were determined by experimental data on the light baryons.<sup>1</sup> The present results seem overall underestimated,

<sup>1</sup>Note that in Ref. [35] the formula for the decay width contains an error. The present results listed in the fourth column are the corrected ones.

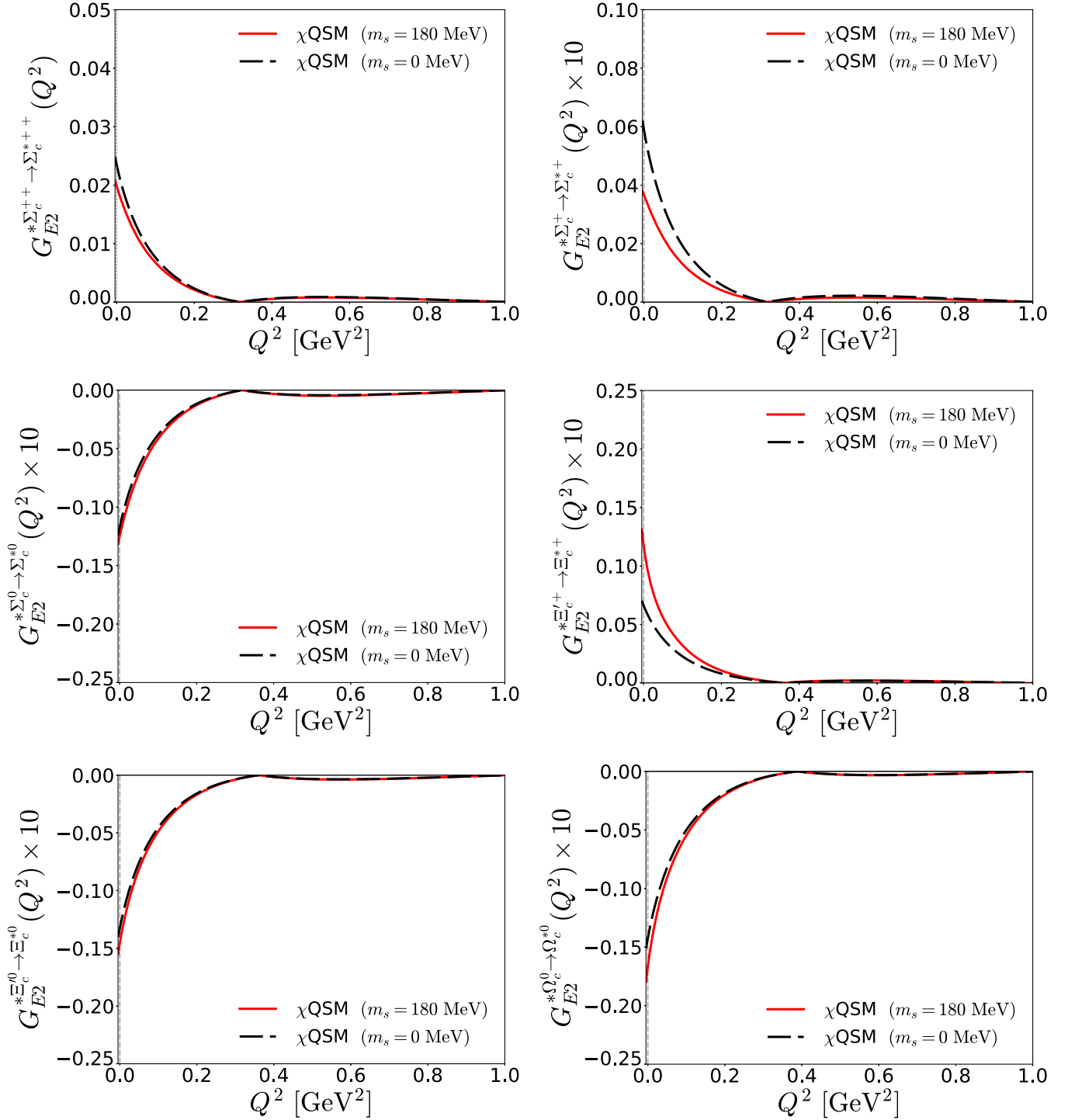


FIG. 8. Results for the electric quadrupole transition form factors from the baryon sextet with spin 1/2 to the baryon sextet with spin 3/2. The notations are the same as in Fig. 6.

compared with those from Ref. [35]. What is interesting is that the present results are in agreement with those from chiral perturbation theory [12]. On the other hand, lattice QCD yields a very small value of the decay width for  $\Omega_c^{*0} \rightarrow \Omega_c^0 \gamma$ , compared with the results from all other works.

We already observed that the E2 transition form factors are very small. This means that the ratios  $R_{EM}$  as defined in Eq. (10) will turn out to be also very small. As listed in Table II, the values of  $R_{EM}$  for the radiative transitions of the baryon sextet with spin 3/2 are indeed very small. Except for the  $\Xi_c^{*+} \gamma \rightarrow \Xi_c^{*+}$  excitation, the values of the

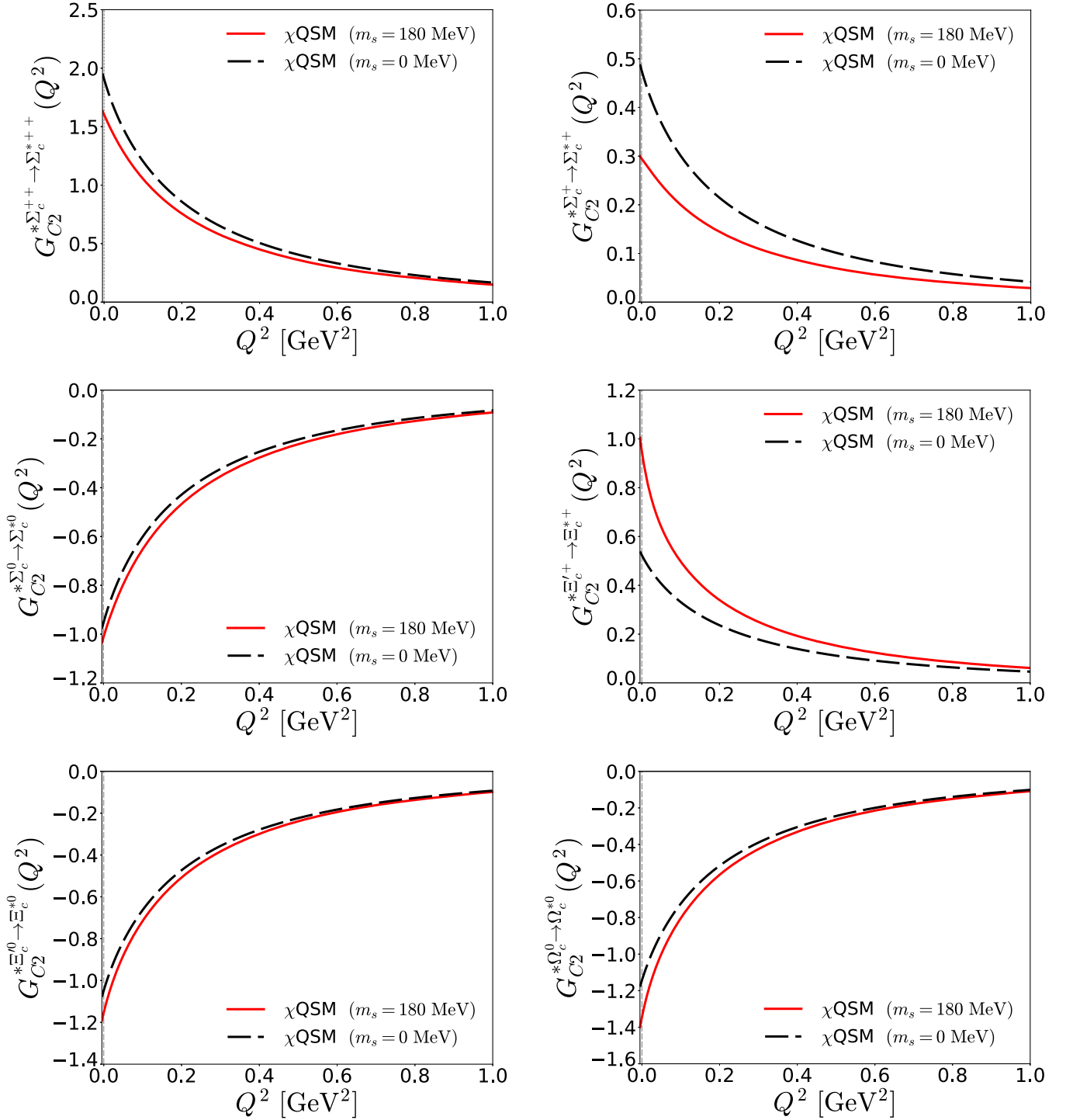


FIG. 9. Results for the Coulomb quadrupole transition form factors from the baryon sextet with spin 1/2 to the baryon sextet with spin 3/2. The notations are the same as in Fig. 6.

ratios  $R_{EM}$  and  $R_{SM}$  are approximately two times smaller than those for the baryon decuplet.

## VI. SUMMARY AND CONCLUSION

We aimed in the present work at investigating the electromagnetic transition form factors for the singly heavy

baryons with spin 3/2, based on the pion mean-field approach or the chiral quark-soliton model. Having taken into account the rotational  $1/N_c$  and linear  $m_s$  corrections, we computed the magnetic dipole, electric quadrupole, and Coulomb quadrupole transition form factors for the radiative excitations from the baryon antitriplet and sextet with spin 1/2 to the baryon sextet with spin 3/2. Since the

TABLE I. Results for the radiative decay widths of  $B\gamma \rightarrow B^*$  with and without flavor SU(3) symmetry breaking, given in units of keV.

$\Gamma(B_c\gamma \rightarrow B_c^*)$	$\chi$ QSM		$\chi$ SM [35]	LQCD [20]	Bag [51]	$\chi$ PT [12]	QCDSR [16,17]	QM [15]
	$(m_s = 0 \text{ MeV})$	$(m_s = 180 \text{ MeV})$						
$\Lambda_c^+\gamma \rightarrow \Sigma_c^{*+}$	63.37	69.76	$191.13 \pm 15.15$	...	126	161.8	130(45)	151(4)
$\Xi_c^+\gamma \rightarrow \Xi_c^{*+}$	34.14	31.97	$55.77 \pm 5.22$	...	44.3	21.6	52(25)	54(3)
$\Xi_c^0\gamma \rightarrow \Xi_c^{*0}$	0	0.08	$1.61 \pm 0.42$	...	0.908	1.84	0.66(32)	0.68(4)
$\Sigma_c^{++}\gamma \rightarrow \Sigma_c^{*++}$	1.12	1.08	$2.41 \pm 0.22$	...	0.826	1.20	2.65(1.20)	...
$\Sigma_c^+\gamma \rightarrow \Sigma_c^{*+}$	0.07	0.06	$0.11 \pm 0.02$	...	0.004	0.04	0.40(16)	0.140(4)
$\Sigma_c^0\gamma \rightarrow \Sigma_c^{*0}$	0.28	0.30	$0.80 \pm 0.06$	...	1.08	0.49	0.08(3)	...
$\Xi_c'^+\gamma \rightarrow \Xi_c^{*+}$	0.09	0.09	$0.21 \pm 0.02$	...	0.011	0.07	0.274	...
$\Xi_c'^0\gamma \rightarrow \Xi_c^{*0}$	0.35	0.34	$0.64 \pm 0.05$	...	1.03	0.42	2.142	...
$\Omega_c^0\gamma \rightarrow \Omega_c^{*0}$	0.38	0.34	$0.49 \pm 0.08$	0.074	1.07	0.32	0.932	...

TABLE II. Results for the  $R_{EM}$  and  $R_{SM}$  on  $B\gamma \rightarrow B^*$  with and without flavor SU(3) symmetry breaking.

	$\chi$ QSM ( $m_s=0\text{MeV}$ )		$\chi$ QSM ( $m_s=180\text{MeV}$ )	
	$R_{EM}[\%]$	$R_{SM}[\%]$	$R_{EM}[\%]$	$R_{SM}[\%]$
$\Sigma_c^{++}\gamma \rightarrow \Sigma_c^{*++}$	-0.87	-0.88	-0.75	-0.76
$\Sigma_c^+\gamma \rightarrow \Sigma_c^{*+}$	-0.87	-0.88	-0.58	-0.59
$\Sigma_c^0\gamma \rightarrow \Sigma_c^{*0}$	-0.87	-0.88	-0.89	-0.91
$\Xi_c'^+\gamma \rightarrow \Xi_c^{*+}$	-0.93	-0.95	-1.63	-1.69
$\Xi_c'^0\gamma \rightarrow \Xi_c^{*0}$	-0.93	-0.95	-1.04	-1.06
$\Omega_c^0\gamma \rightarrow \Omega_c^{*0}$	-0.96	-0.98	-1.19	-1.22

model parameters were already fixed in producing properties of the light baryons, we use exactly the same set of the parameters for the present investigation. We compared the results for the magnetic dipole and electric quadrupole transition form factors with those from a lattice calculation. However, the lattice results for the form factor for the  $\Omega_c^0 \rightarrow \Omega_c^{*0}$  M1 transition seems to be underestimated in comparison with those from other works. Since the lattice calculation suffers from large uncertainties in the results for the corresponding E2 transition form factor, we were not able to draw any conclusion from the comparison of the present results with the lattice ones. We then examined the valence- and sea-quark contributions to the M1, E2, and C2 transition form factors. While the sea-quark contributions are marginal to the M1 form factors, they dominate over the valence-quark contributions in the smaller  $Q^2$  region. On the other hand, the sea-quark contributions fall off faster than the valence-quark ones as  $Q^2$  increases. The magnitudes of the M1 transitions form factors from the baryon antitriplet to the baryon sextet with spin 3/2 are in general larger than those from the baryon sextet with spin 1/2 to the sextet with spin 3/2. This indicates that the M1 transitions occur more naturally between the states with the total spin flipped. Since the E2 and C2 transitions take place in the transitions without any spin flip, we have null results for the transitions from the baryon antitriplet to the sextet with spin 3/2.

We also examined the effects of flavor SU(3) symmetry breaking by considering the linear  $m_s$  corrections. Except for the  $\Xi_c^0 \rightarrow \Xi_c^{*0}$  transition that is forbidden by the  $U$ -spin symmetry, we found that the effects of the flavor SU(3) symmetry breaking are negligibly small. Since the  $U$ -spin symmetry is broken by the finite value of the strange current quark mass, the M1 transition form factor for the  $\Xi_c^0 \rightarrow \Xi_c^{*0}$  radiative excitation is finite but tiny, compared with those for other transition modes. Similarly, we found that the linear  $m_s$  corrections yield also very small contribution to the E2 transition form factors except for the  $\Sigma_c^+ \rightarrow \Sigma_c^{*+}$  and  $\Xi_c'^+ \rightarrow \Xi_c^{*+}$  transitions. Similar features were seen in the results for Coulomb quadrupole form factors. We also computed the widths of the radiative decays for the baryon sextet with spin 3/2. The results for the transitions within the baryon sextet are in agreement with those from chiral perturbation theory. Finally, we presented the results for the ratios of the E2 over M1 and C2 over M1. They turn out to be approximately two times smaller than those for the baryon decuplet. As the electromagnetic (transition) form factors provide the most valuable information on the structure of the hadrons, it is extremely important to measure them, experimentally and/or by lattice QCD computations. So far, very limited information is given for the charmed baryons, and further experimental and computational efforts are highly desired.

## ACKNOWLEDGMENTS

The authors are grateful to K. U. Can for valuable discussion related to the lattice results. The present work was supported by Basic Science Research Program through the National Research Foundation of Korea funded by the Ministry of Education, Science and Technology (Grants No. 2018R1A2B2001752 and No. 2018R1A5A1025563). J.-Y. K is supported by the Deutscher Akademischer Austauschdienst (DAAD) doctoral scholarship. The work of Gh.-S.-Y. is supported by Basic Science Research Program through the National Research Foundation of

Korea funded by the Ministry of Education, Science and Technology (Grant No. NRF- 2019R1A2C1010443). The work of M. O. is supported in part by JSPS KAKENHI Grants No. JP19H05159 and No. JP20K03959.

## APPENDIX A: DENSITIES FOR THE EM TRANSITION FORM FACTORS

The densities of the magnetic dipole transition form factors are expressed explicitly as follows:

$$\begin{aligned}
\mathcal{Q}_0(\mathbf{r}) &= (N_c - 1) \langle \text{val} | \mathbf{r} \rangle \gamma^5 \{ \hat{\mathbf{r}} \times \boldsymbol{\sigma} \} \cdot \boldsymbol{\tau} \langle \mathbf{r} | \text{val} \rangle + N_c \sum_n \mathcal{R}_1(E_n) \langle n | \mathbf{r} \rangle \gamma^5 \{ \hat{\mathbf{r}} \times \boldsymbol{\sigma} \} \cdot \boldsymbol{\tau} \langle \mathbf{r} | n \rangle, \\
\mathcal{Q}_1(\mathbf{r}) &= \frac{i}{2} (N_c - 1) \sum_{n \neq \text{val}} \frac{\text{sign}(E_n)}{E_n - E_{\text{val}}} \langle n | \mathbf{r} \rangle \gamma^5 \{ \{ \hat{\mathbf{r}} \times \boldsymbol{\sigma} \} \times \boldsymbol{\tau} \} \langle \mathbf{r} | \text{val} \rangle \cdot \langle \text{val} | \boldsymbol{\tau} | n \rangle \\
&\quad + \frac{i}{4} N_c \sum_{n,m} \mathcal{R}_4(E_n, E_m) \langle m | \mathbf{r} \rangle \gamma^5 \{ \{ \hat{\mathbf{r}} \times \boldsymbol{\sigma} \} \times \boldsymbol{\tau} \} \langle \mathbf{r} | n \rangle \cdot \langle m | \boldsymbol{\tau} | n \rangle, \\
\mathcal{X}_1(\mathbf{r}) &= (N_c - 1) \sum_{n \neq \text{val}} \frac{1}{E_n - E_{\text{val}}} \langle \text{val} | \mathbf{r} \rangle \gamma^5 \{ \hat{\mathbf{r}} \times \boldsymbol{\sigma} \} \langle \mathbf{r} | \text{val} \rangle \cdot \langle n | \boldsymbol{\tau} | \text{val} \rangle + \frac{1}{2} N_c \sum_{n,m} \mathcal{R}_5(E_n, E_m) \langle n | \mathbf{r} \rangle \gamma^5 \{ \hat{\mathbf{r}} \times \boldsymbol{\sigma} \} \langle \mathbf{r} | m \rangle \cdot \langle m | \boldsymbol{\tau} | n \rangle, \\
\mathcal{X}_2(\mathbf{r}) &= (N_c - 1) \sum_{n^0} \frac{1}{E_{n^0} - E_{\text{val}}} \langle \text{val} | \mathbf{r} \rangle \gamma^5 \{ \hat{\mathbf{r}} \times \boldsymbol{\sigma} \} \cdot \boldsymbol{\tau} \langle \mathbf{r} | n^0 \rangle \langle n^0 | \text{val} \rangle + N_c \sum_{n^0,m} \mathcal{R}_5(E_m, E_{n^0}) \langle m | \mathbf{r} \rangle \gamma^5 \{ \hat{\mathbf{r}} \times \boldsymbol{\sigma} \} \cdot \boldsymbol{\tau} \langle \mathbf{r} | n^0 \rangle \langle n^0 | m \rangle, \\
\mathcal{M}_0(\mathbf{r}) &= (N_c - 1) \sum_{n \neq \text{val}} \frac{1}{E_n - E_{\text{val}}} \langle \text{val} | \mathbf{r} \rangle \gamma^5 \{ \hat{\mathbf{r}} \times \boldsymbol{\sigma} \} \cdot \boldsymbol{\tau} \langle \mathbf{r} | n \rangle \langle n | \gamma^0 | \text{val} \rangle \\
&\quad - \frac{1}{2} N_c \sum_{n,m} \mathcal{R}_2(E_n, E_m) \langle m | \mathbf{r} \rangle \gamma^5 \{ \hat{\mathbf{r}} \times \boldsymbol{\sigma} \} \cdot \boldsymbol{\tau} \langle \mathbf{r} | n \rangle \langle n | \gamma^0 | m \rangle, \\
\mathcal{M}_1(\mathbf{r}) &= (N_c - 1) \sum_{n \neq \text{val}} \frac{1}{E_n - E_{\text{val}}} \langle \text{val} | \mathbf{r} \rangle \gamma^5 \{ \hat{\mathbf{r}} \times \boldsymbol{\sigma} \} \langle \mathbf{r} | n \rangle \cdot \langle n | \gamma^0 \boldsymbol{\tau} | \text{val} \rangle \\
&\quad - \frac{1}{2} N_c \sum_{n,m} \mathcal{R}_2(E_n, E_m) \langle m | \mathbf{r} \rangle \gamma^5 \{ \hat{\mathbf{r}} \times \boldsymbol{\sigma} \} \langle \mathbf{r} | n \rangle \cdot \langle n | \gamma^0 \boldsymbol{\tau} | m \rangle, \\
\mathcal{M}_2(\mathbf{r}) &= (N_c - 1) \sum_{n^0} \frac{1}{E_{n^0} - E_{\text{val}}} \langle \text{val} | \mathbf{r} \rangle \gamma^5 \{ \hat{\mathbf{r}} \times \boldsymbol{\sigma} \} \cdot \boldsymbol{\tau} \langle \mathbf{r} | n^0 \rangle \langle n^0 | \gamma^0 | \text{val} \rangle \\
&\quad - N_c \sum_{n^0,m} \mathcal{R}_2(E_{n^0}, E_m) \langle m | \mathbf{r} \rangle \gamma^5 \{ \hat{\mathbf{r}} \times \boldsymbol{\sigma} \} \cdot \boldsymbol{\tau} \langle \mathbf{r} | n^0 \rangle \langle n^0 | \gamma^0 | m \rangle. \tag{A1}
\end{aligned}$$

The densities of the electric quadrupole transition form factors are given as

$$\begin{aligned}
-2\sqrt{10} \mathcal{I}_{1E2}(\mathbf{r}) &= (N_c - 1) \sum_{n \neq \text{val}} \frac{1}{E_n - E_{\text{val}}} \langle \text{val} | \boldsymbol{\tau} | n \rangle \cdot \langle n | \mathbf{r} \rangle \{ \sqrt{4\pi} Y_2 \otimes \tau_1 \}_1 \langle \mathbf{r} | \text{val} \rangle \\
&\quad + \frac{1}{2} N_c \sum_{n,m} \mathcal{R}_3(E_n, E_m) \langle n | \boldsymbol{\tau} | m \rangle \cdot \langle m | \mathbf{r} \rangle \{ \sqrt{4\pi} Y_2 \otimes \tau_1 \}_1 \langle \mathbf{r} | n \rangle, \\
-2\sqrt{10} \mathcal{K}_{1E2}(\mathbf{r}) &= (N_c - 1) \sum_{n \neq \text{val}} \frac{1}{E_n - E_{\text{val}}} \langle \text{val} | \gamma^0 \boldsymbol{\tau} | n \rangle \cdot \langle n | \mathbf{r} \rangle \{ \sqrt{4\pi} Y_2 \otimes \tau_1 \}_1 \langle \mathbf{r} | \text{val} \rangle \\
&\quad + \frac{1}{2} N_c \sum_{n,m} \mathcal{R}_5(E_n, E_m) \langle n | \gamma^0 \boldsymbol{\tau} | m \rangle \cdot \langle m | \mathbf{r} \rangle \{ \sqrt{4\pi} Y_2 \otimes \tau_1 \}_1 \langle \mathbf{r} | n \rangle. \tag{A2}
\end{aligned}$$

The regularization functions in Eqs. (A1) and (A2) are defined by

$$\begin{aligned}
\mathcal{R}_1(E_n) &= -\frac{1}{2\sqrt{\pi}} E_n \int_0^\infty \phi(u) \frac{du}{u} e^{-uE_n^2}, \\
\mathcal{R}_2(E_n, E_m) &= \frac{1}{2\sqrt{\pi}} \int_0^\infty \phi(u) \frac{du}{\sqrt{u}} \frac{E_m e^{-uE_m^2} - E_n e^{-uE_n^2}}{E_n - E_m}, \\
\mathcal{R}_3(E_n, E_m) &= \frac{1}{2\sqrt{\pi}} \int_0^\infty \phi(u) \frac{du}{\sqrt{u}} \left[ \frac{e^{-uE_m^2} - e^{-uE_n^2}}{u(E_n^2 - E_m^2)} - \frac{E_m e^{-uE_m^2} + E_n e^{-uE_n^2}}{E_n + E_m} \right], \\
\mathcal{R}_4(E_n, E_m) &= \frac{1}{2\pi} \int_0^\infty \phi(u) du \int_0^1 d\alpha e^{-uE_n^2(1-\alpha) - uE_m^2\alpha} \frac{E_n(1-\alpha) - \alpha E_m}{\sqrt{\alpha(1-\alpha)}}, \\
\mathcal{R}_5(E_n, E_m) &= \frac{\text{sign}(E_n) - \text{sign}(E_m)}{2(E_n - E_m)},
\end{aligned} \tag{A3}$$

with proper-time regulator  $\phi(u) = c\theta(u - \Lambda_1^{-2}) + (1-c)\theta(u - \Lambda_2^{-2})$ . The cutoff parameters  $c, \Lambda_1$ , and  $\Lambda_2$  were determined in Ref. [42].  $|val\rangle$  and  $|n\rangle$  denote the states of the valence and sea quarks with the corresponding eigenenergies  $E_{val}$  and  $E_n$  of the single-quark Hamiltonian  $h(U_c)$ , respectively [42].

## APPENDIX B: COLLECTIVE MATRIX ELEMENTS OF ELECTROMAGNETIC FORM FACTOR

In Tables III, IV, V, and VI, we present the results for all relevant matrix elements of the SU(3) Wigner  $D$  functions.

TABLE III. The matrix elements of the collective operators for the leading-order contributions and the  $1/N_c$  rotational corrections to the electromagnetic transition form factors.

$B_3\gamma^* \rightarrow B_6$	$\Lambda_c\gamma^* \rightarrow \Sigma_c^*$	$\Xi_c\gamma^* \rightarrow \Xi_c^*$	$B_6\gamma^* \rightarrow B_6$	$\Sigma_c\gamma^* \rightarrow \Sigma_c^*$	$\Xi_c'\gamma^* \rightarrow \Xi_c^*$	$\Omega_c\gamma^* \rightarrow \Omega_c^*$
$\langle B_6   D_{33}^{(8)}   B_3 \rangle$	$\frac{1}{2\sqrt{3}}$	$-\frac{1}{2\sqrt{3}} T_3$	$\langle B_6   D_{33}^{(8)}   B_6 \rangle$	$\frac{1}{5\sqrt{2}} T_3$	$\frac{1}{5\sqrt{2}} T_3$	0
$\langle B_6   D_{83}^{(8)}   B_3 \rangle$	0	$-\frac{1}{4}$	$\langle B_6   D_{83}^{(8)}   B_6 \rangle$	$\frac{1}{5\sqrt{6}}$	$-\frac{1}{10\sqrt{6}}$	$-\frac{1}{5}\sqrt{\frac{2}{3}}$
$\langle B_6   D_{38}^{(8)} J_3   B_3 \rangle$	0	0	$\langle B_6   D_{38}^{(8)} J_3   B_6 \rangle$	$-\frac{1}{5\sqrt{6}} T_3$	$-\frac{1}{5\sqrt{6}} T_3$	0
$\langle B_6   D_{88}^{(8)} J_3   B_3 \rangle$	0	0	$\langle B_6   D_{88}^{(8)} J_3   B_6 \rangle$	$-\frac{1}{15\sqrt{2}}$	$\frac{1}{30\sqrt{2}}$	$\frac{\sqrt{2}}{15}$
$\langle B_6   d_{ab3} D_{3a}^{(8)} J_b   B_3 \rangle$	$-\frac{1}{4\sqrt{3}}$	$\frac{1}{4\sqrt{3}} T_3$	$\langle B_6   d_{ab3} D_{3a}^{(8)} J_b   B_6 \rangle$	$-\frac{1}{10\sqrt{2}} T_3$	$-\frac{1}{10\sqrt{2}} T_3$	0
$\langle B_6   d_{ab3} D_{8a}^{(8)} J_b   B_3 \rangle$	0	$\frac{1}{8}$	$\langle B_6   d_{ab3} D_{8a}^{(8)} J_b   B_6 \rangle$	$-\frac{1}{10\sqrt{6}}$	$\frac{1}{20\sqrt{6}}$	$\frac{1}{5\sqrt{6}}$
$\langle B_6   D_{3i}^{(8)} J_i   B_3 \rangle$	0	0	$\langle B_6   D_{3i}^{(8)} J_i   B_6 \rangle$	0	0	0
$\langle B_6   D_{8i}^{(8)} J_i   B_3 \rangle$	0	0	$\langle B_6   D_{8i}^{(8)} J_i   B_6 \rangle$	0	0	0

TABLE IV. The matrix elements of the collective operators for the  $m_s$  corrections to the electromagnetic transition form factors.

$B_3\gamma^* \rightarrow B_6$	$\Lambda_c\gamma^* \rightarrow \Sigma_c^*$	$\Xi_c\gamma^* \rightarrow \Xi_c^*$	$B_6\gamma^* \rightarrow B_6$	$\Sigma_c\gamma^* \rightarrow \Sigma_c^*$	$\Xi_c'\gamma^* \rightarrow \Xi_c^*$	$\Omega_c\gamma^* \rightarrow \Omega_c^*$
$\langle B_6   D_{88}^{(8)} D_{33}^{(8)}   B_3 \rangle$	$\frac{\sqrt{3}}{20}$	0	$\langle B_6   D_{88}^{(8)} D_{33}^{(8)}   B_6 \rangle$	$\frac{\sqrt{2}}{45} T_3$	$\frac{1}{45\sqrt{2}} T_3$	0
$\langle B_6   D_{88}^{(8)} D_{83}^{(8)}   B_3 \rangle$	0	$\frac{1}{20}$	$\langle B_6   D_{88}^{(8)} D_{83}^{(8)}   B_6 \rangle$	$-\frac{1}{30\sqrt{6}}$	0	$\frac{1}{10\sqrt{6}}$
$\langle B_6   D_{83}^{(8)} D_{38}^{(8)}   B_3 \rangle$	$\frac{1}{20\sqrt{3}}$	$-\frac{1}{5\sqrt{3}} T_3$	$\langle B_6   D_{83}^{(8)} D_{38}^{(8)}   B_6 \rangle$	$\frac{\sqrt{2}}{45} T_3$	$\frac{1}{45\sqrt{2}} T_3$	0
$\langle B_6   D_{83}^{(8)} D_{88}^{(8)}   B_3 \rangle$	0	$\frac{1}{20}$	$\langle B_6   D_{83}^{(8)} D_{88}^{(8)}   B_6 \rangle$	$-\frac{1}{30\sqrt{6}}$	0	$\frac{1}{10\sqrt{6}}$
$\langle B_6   d_{ab3} D_{8a}^{(8)} D_{8b}^{(8)}   B_3 \rangle$	0	$\frac{\sqrt{3}}{20}$	$\langle B_6   d_{ab3} D_{8a}^{(8)} D_{8b}^{(8)}   B_6 \rangle$	$-\frac{\sqrt{2}}{45}$	$\frac{1}{30\sqrt{2}}$	$\frac{1}{15\sqrt{2}}$
$\langle B_6   d_{ab3} D_{3a}^{(8)} D_{8b}^{(8)}   B_3 \rangle$	$\frac{1}{10}$	$-\frac{1}{10} T_3$	$\langle B_6   d_{ab3} D_{3a}^{(8)} D_{8b}^{(8)}   B_6 \rangle$	$\frac{1}{9\sqrt{6}} T_3$	$\frac{7}{45\sqrt{6}} T_3$	0
$\langle B_6   D_{83}^{(8)} D_{33}^{(8)}   B_3 \rangle$	0	0	$\langle B_6   D_{83}^{(8)} D_{33}^{(8)}   B_6 \rangle$	$-\frac{1}{45}\sqrt{\frac{2}{3}} T_3$	$\frac{4}{45}\sqrt{\frac{2}{3}} T_3$	0
$\langle B_6   D_{83}^{(8)} D_{83}^{(8)}   B_3 \rangle$	0	0	$\langle B_6   D_{83}^{(8)} D_{83}^{(8)}   B_6 \rangle$	$-\frac{1}{45\sqrt{2}}$	$\frac{1}{15\sqrt{2}}$	$-\frac{1}{15\sqrt{2}}$
$\langle B_6   D_{8i}^{(8)} D_{3i}^{(8)}   B_3 \rangle$	0	0	$\langle B_6   D_{8i}^{(8)} D_{3i}^{(8)}   B_6 \rangle$	$\frac{1}{45}\sqrt{\frac{2}{3}} T_3$	$-\frac{4}{45}\sqrt{\frac{2}{3}} T_3$	0
$\langle B_6   D_{8i}^{(8)} D_{8i}^{(8)}   B_3 \rangle$	0	0	$\langle B_6   D_{8i}^{(8)} D_{8i}^{(8)}   B_6 \rangle$	$\frac{1}{45\sqrt{2}}$	$-\frac{1}{15\sqrt{2}}$	$\frac{1}{15\sqrt{2}}$

TABLE V. The relevant transition matrix elements of the collective operators coming from the 15-plet component of the baryon wave functions.

$B_{\overline{15}}\gamma^* \rightarrow B_6$	$\Lambda_c\gamma^* \rightarrow \Sigma_c^*$	$\Xi_c\gamma^* \rightarrow \Xi_c^*$	$B_{\overline{15}}\gamma^* \rightarrow B_6$	$\Sigma_c\gamma^* \rightarrow \Sigma_c^*$	$\Xi_c'\gamma^* \rightarrow \Xi_c^*$	$\Omega_c\gamma^* \rightarrow \Omega_c^*$
$\langle B_6   D_{33}^{(8)}   B_{\overline{15}} \rangle$	$\frac{1}{6\sqrt{15}}$	$-\frac{\sqrt{5}}{18} T_3$	$\langle B_6   D_{33}^{(8)}   B_{\overline{15}} \rangle$	$\frac{1}{9\sqrt{5}} T_3$	$\frac{1}{9} \sqrt{\frac{5}{6}} T_3$	0
$\langle B_6   D_{83}^{(8)}   B_{\overline{15}} \rangle$	0	$\frac{1}{4\sqrt{15}}$	$\langle B_6   D_{83}^{(8)}   B_{\overline{15}} \rangle$	$-\frac{1}{3\sqrt{15}}$	$-\frac{1}{6\sqrt{10}}$	0
$\langle B_6   D_{38}^{(8)} J_3   B_{\overline{15}} \rangle$	0	0	$\langle B_6   D_{38}^{(8)} J_3   B_{\overline{15}} \rangle$	$\frac{1}{3\sqrt{15}} T_3$	$\frac{1}{9} \sqrt{\frac{5}{2}} T_3$	0
$\langle B_6   D_{88}^{(8)} J_3   B_{\overline{15}} \rangle$	0	0	$\langle B_6   D_{88}^{(8)} J_3   B_{\overline{15}} \rangle$	$-\frac{1}{3\sqrt{5}}$	$-\frac{1}{2\sqrt{30}}$	0
$\langle B_6   d_{ab3} D_{3a}^{(8)} J_b   B_{\overline{15}} \rangle$	$\frac{1}{4\sqrt{15}}$	$-\frac{\sqrt{5}}{12} T_3$	$\langle B_6   d_{ab3} D_{3a}^{(8)} J_b   B_{\overline{15}} \rangle$	$\frac{1}{18\sqrt{5}} T_3$	$\frac{1}{18} \sqrt{\frac{5}{6}} T_3$	0
$\langle B_6   d_{ab3} D_{8a}^{(8)} J_b   B_{\overline{15}} \rangle$	0	$\frac{1}{8} \sqrt{\frac{3}{5}}$	$\langle B_6   d_{ab3} D_{8a}^{(8)} J_b   B_{\overline{15}} \rangle$	$-\frac{1}{6\sqrt{15}}$	$-\frac{1}{12\sqrt{10}}$	0
$\langle B_6   D_{3i}^{(8)} J_i   B_{\overline{15}} \rangle$	0	0	$\langle B_6   D_{3i}^{(8)} J_i   B_{\overline{15}} \rangle$	0	0	0
$\langle B_6   D_{8i}^{(8)} J_i   B_{\overline{15}} \rangle$	0	0	$\langle B_6   D_{8i}^{(8)} J_i   B_{\overline{15}} \rangle$	0	0	0

TABLE VI. The relevant transition matrix elements of the collective operators coming from the 15- and 24-plet components of the baryon wave functions.

$B_{\overline{3}}\gamma^* \rightarrow B_{\overline{15}}$	$\Lambda_c\gamma^* \rightarrow \Sigma_c^*$	$\Xi_c\gamma^* \rightarrow \Xi_c^*$	$B_6\gamma^* \rightarrow B_{\overline{24}}$	$\Sigma_c\gamma^* \rightarrow \Sigma_c^*$	$\Xi_c'\gamma^* \rightarrow \Xi_c^*$	$\Omega_c\gamma^* \rightarrow \Omega_c^*$
$\langle B_{\overline{15}}   D_{33}^{(8)}   B_{\overline{3}} \rangle$	$\frac{1}{\sqrt{30}}$	$-\frac{\sqrt{5}}{6} T_3$	$\langle B_{\overline{24}}   D_{33}^{(8)}   B_6 \rangle$	$\frac{1}{90\sqrt{2}} T_3$	$\frac{1}{45\sqrt{3}} T_3$	0
$\langle B_{\overline{15}}   D_{83}^{(8)}   B_{\overline{3}} \rangle$	0	$\frac{1}{4} \sqrt{\frac{3}{5}}$	$\langle B_{\overline{24}}   D_{83}^{(8)}   B_6 \rangle$	$\frac{1}{15\sqrt{6}}$	$\frac{1}{30}$	$\frac{1}{30}$
$\langle B_{\overline{15}}   D_{38}^{(8)} J_3   B_{\overline{3}} \rangle$	0	0	$\langle B_{\overline{24}}   D_{38}^{(8)} J_3   B_6 \rangle$	$-\frac{1}{15\sqrt{6}} T_3$	$-\frac{2}{45} T_3$	0
$\langle B_{\overline{15}}   D_{88}^{(8)} J_3   B_{\overline{3}} \rangle$	0	0	$\langle B_{\overline{24}}   D_{88}^{(8)} J_3   B_6 \rangle$	$-\frac{\sqrt{2}}{15}$	$-\frac{1}{5\sqrt{3}}$	$-\frac{1}{5\sqrt{3}}$
$\langle B_{\overline{15}}   d_{ab3} D_{3a}^{(8)} J_b   B_{\overline{3}} \rangle$	$\frac{1}{2\sqrt{30}}$	$-\frac{1}{12\sqrt{5}} T_3$	$\langle B_{\overline{24}}   d_{ab3} D_{3a}^{(8)} J_b   B_6 \rangle$	$\frac{1}{45\sqrt{2}} T_3$	$\frac{2}{45\sqrt{3}} T_3$	0
$\langle B_{\overline{15}}   d_{ab3} D_{8a}^{(8)} J_b   B_{\overline{3}} \rangle$	0	$\frac{1}{8} \sqrt{\frac{3}{5}}$	$\langle B_{\overline{24}}   d_{ab3} D_{8a}^{(8)} J_b   B_6 \rangle$	$\frac{1}{15} \sqrt{\frac{2}{3}}$	$\frac{1}{15}$	$\frac{1}{15}$
$\langle B_{\overline{15}}   D_{3i}^{(8)} J_i   B_{\overline{3}} \rangle$	0	0	$\langle B_{\overline{24}}   D_{3i}^{(8)} J_i   B_6 \rangle$	0	0	0
$\langle B_{\overline{15}}   D_{8i}^{(8)} J_i   B_{\overline{3}} \rangle$	0	0	$\langle B_{\overline{24}}   D_{8i}^{(8)} J_i   B_6 \rangle$	0	0	0

- [1] A. J. Buchmann and E. M. Henley, *Phys. Rev. C* **63**, 015202 (2000).
- [2] S. Kumano, *Phys. Lett. B* **214**, 132 (1988).
- [3] M. N. Butler, M. J. Savage, and R. P. Springer, *Phys. Lett. B* **304**, 353 (1993).
- [4] C. P. Jessop *et al.* (CLEO Collaboration), *Phys. Rev. Lett.* **82**, 492 (1999).
- [5] B. Aubert *et al.* (BABAR Collaboration), *Phys. Rev. Lett.* **97**, 232001 (2006).
- [6] E. Solovieva *et al.*, *Phys. Lett. B* **672**, 1 (2009).
- [7] J. Yelton *et al.* (Belle Collaboration), *Phys. Rev. D* **94**, 052011 (2016).
- [8] H. Y. Cheng, C. Y. Cheung, G. L. Lin, Y. C. Lin, T. M. Yan, and H. L. Yu, *Phys. Rev. D* **47**, 1030 (1993).
- [9] M. J. Savage, *Phys. Lett. B* **345**, 61 (1995).
- [10] S. L. Zhu and Y. B. Dai, *Phys. Rev. D* **59**, 114015 (1999).
- [11] M. C. Banuls, A. Pich, and I. Scimemi, *Phys. Rev. D* **61**, 094009 (2000).
- [12] G. J. Wang, L. Meng, and S. L. Zhu, *Phys. Rev. D* **99**, 034021 (2019).
- [13] J. Dey, V. Shevchenko, P. Volkovitsky, and M. Dey, *Phys. Lett. B* **337**, 185 (1994).
- [14] S. Tawfiq, J. G. Korner, and P. J. O'Donnell, *Phys. Rev. D* **63**, 034005 (2001).
- [15] M. A. Ivanov, J. G. Korner, V. E. Lyubovitskij, and A. G. Rusetsky, *Phys. Rev. D* **60**, 094002 (1999).
- [16] T. M. Aliev, K. Azizi, and A. Ozpineci, *Phys. Rev. D* **79**, 056005 (2009).
- [17] T. M. Aliev, K. Azizi, and H. Sundu, *Eur. Phys. J. C* **75**, 14 (2015).
- [18] T. M. Aliev, T. Barakat, and M. Savcı, *Phys. Rev. D* **93**, 056007 (2016).

- [19] H. Y. Cheng, *Front. Phys. (Beijing)* **10**, 101406 (2015).
- [20] H. Bahtiyar, K. U. Can, G. Erkol, and M. Oka, *Phys. Lett. B* **747**, 281 (2015).
- [21] H. Bahtiyar, K. U. Can, G. Erkol, M. Oka, and T. T. Takahashi, *J. Phys. Soc. Jpn. Conf. Proc.* **26**, 022027 (2019).
- [22] E. Witten, *Nucl. Phys.* **B160**, 57 (1979).
- [23] D. Diakonov, V. Y. Petrov, and P. V. Pobylitsa, *Nucl. Phys.* **B306**, 809 (1988).
- [24] A. Blotz, D. Diakonov, K. Goeke, N. W. Park, V. Petrov, and P. V. Pobylitsa, *Nucl. Phys.* **A555**, 765 (1993).
- [25] G. S. Yang, H.-Ch. Kim, M. V. Polyakov, and M. Praszalowicz, *Phys. Rev. D* **94**, 071502R (2016).
- [26] J. Y. Kim, H.-Ch. Kim, and G. S. Yang, *Phys. Rev. D* **98**, 054004 (2018).
- [27] J. Y. Kim and H.-Ch. Kim, *Prog. Theor. Exp. Phys.* **2020**, 043D03 (2020).
- [28] D. Diakonov, arXiv:1003.2157.
- [29] N. Isgur and M. B. Wise, *Phys. Lett. B* **232**, 113 (1989).
- [30] N. Isgur and M. B. Wise, *Phys. Rev. Lett.* **66**, 1130 (1991).
- [31] H. Georgi, *Phys. Lett. B* **240**, 447 (1990).
- [32] H.-Ch. Kim, M. V. Polyakov, and M. Praszalowicz, *Phys. Rev. D* **96**, 014009 (2017); **96**, A039902 (2017).
- [33] H.-Ch. Kim, M. V. Polyakov, M. Praszalowicz, and G. S. Yang, *Phys. Rev. D* **96**, 094021 (2017); **97**, 039901(E) (2018).
- [34] G. S. Yang and H.-Ch. Kim, *Phys. Lett. B* **808**, 135619 (2020).
- [35] G. S. Yang and H.-Ch. Kim, *Phys. Lett. B* **801**, 135142 (2020).
- [36] H.-Ch. Kim, *J. Korean Phys. Soc.* **73**, 165 (2018).
- [37] J. Y. Kim and H.-Ch. Kim, *Phys. Rev. D* **97**, 114009 (2018).
- [38] J. Y. Kim and H.-Ch. Kim, *Prog. Theor. Exp. Phys.* **(2021)**, 023D02 (2021).
- [39] J. Y. Kim and H.-Ch. Kim, arXiv:1912.01437.
- [40] M. Tanabashi *et al.* (Particle Data Group), *Phys. Rev. D* **98**, 030001 (2018).
- [41] M. A. Shifman, in *ITEP Lectures on Particle Physics and Field Theory*, edited by M. A. Shifman (World Scientific, Singapore, 1995), Vol. 1, pp. 1–109.
- [42] C. V. Christov, A. Blotz, H. C. Kim, P. Pobylitsa, T. Watabe, T. Meissner, E. Ruiz Arriola, and K. Goeke, *Prog. Part. Nucl. Phys.* **37**, 91 (1996).
- [43] T. Ledwig, A. Silva, and M. Vanderhaeghen, *Phys. Rev. D* **79**, 094025 (2009).
- [44] J. Y. Kim and H.-Ch. Kim, *Eur. Phys. J. C* **79**, 570 (2019).
- [45] H.-Ch. Kim, A. Blotz, M. V. Polyakov, and K. Goeke, *Phys. Rev. D* **53**, 4013 (1996).
- [46] P. L. Cho and H. Georgi, *Phys. Lett. B* **296**, 408 (1992); **300**, 410(E) (1993).
- [47] A. J. Buchmann, J. A. Hester, and R. F. Lebed, *Phys. Rev. D* **66**, 056002 (2002).
- [48] K. U. Can, G. Erkol, M. Oka, and T. T. Takahashi, *Phys. Rev. D* **92**, 114515 (2015).
- [49] K. Goeke, J. Grabis, J. Ossmann, M. V. Polyakov, P. Schweitzer, A. Silva, and D. Urbano, *Phys. Rev. D* **75**, 094021 (2007).
- [50] J. Y. Kim and H.-Ch. Kim, *Eur. Phys. J. C* **80**, 1087 (2020).
- [51] A. Bernotas and V. Šimonis, *Phys. Rev. D* **87**, 074016 (2013).